NASA TECHNICAL NOTE

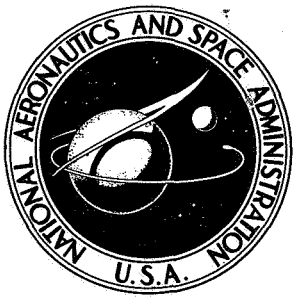

NASA TN D-7252

NASA TN D-7252

RESULTS OF FULL-SCALE WIND TUNNEL TESTS ON THE H.126 JET FLAP AIRCRAFT

by Thomas N. Aiken and Anthony M. Cook

Ames Research Center
Moffett Field, Calif. 94035

NATIONAL AERONAUTICS AND SPACE ADMINISTRATION • WASHINGTON, D. C. • APRIL 1973

1. Report No.	2. Government Accession No.	3. Recipient's Catalog No.
NASA TN D-7252		

4. Title and Subtitle	5. Report Date
RESULTS OF FULL-SCALE WIND TUNNEL TESTS ON THE H.126 JET FLAP AIRCRAFT	April 1973
	6. Performing Organization Code
7. Author(s)	8. Performing Organization Report No.
Thomas N. Aiken and Anthony M. Cook	A-3611
	10. Work Unit No.
9. Performing Organization Name and Address	126–13–01–39–00–21
NASA Ames Research Center Moffett Field, Calif., 94035	11. Contract or Grant No.
	13. Type of Report and Period Covered
12. Sponsoring Agency Name and Address	Technical Memorandum
National Aeronautics and Space Administration Washington, D. C., 20546	14. Sponsoring Agency Code

15. Supplementary Notes

16. Abstract

The aerodynamic characteristics of the full-scale H.126 jet flap aircraft were studied in the Ames 40- by 80-Foot Wind Tunnel. The H.126 aircraft is designed for research on flight characteristics of an aircraft using the jet flap principle.

Static longitudinal, lateral, and directional characteristics were measured at a Reynolds number of 2.5 to 2.7 million. The jet control power as well as the aerodynamic characteristics were measured and are presented herein with limited discussion. The primary configuration variables were flap and aileron deflection.

17. Key Words (Suggested by Author(s))	18. Distribution Statement
STOL Jet Flap High-Lift Wing	Unclassified – Unlimited

19. Security Classif. (of this report)	20. Security Classif. (of this page)	21. No. of Pages	22. Price*
Unclassified	Unclassified	66	$3.00

* For sale by the National Technical Information Service, Springfield, Virginia 22151

NOTATION

b	wing span, m (ft)
c	wing chord, m (ft)
$\overline{c}$	wing mean aerodynamic chord, m (ft)
C_D	drag coefficient, $\frac{\text{net drag}}{qS}$
C_J	jet momentum coefficient of wing, $\frac{X_{GW}}{qS}$
C_l	rolling-moment coefficient, $\frac{\text{rolling moment}}{qSb}$
C_L	lift coefficient, $\frac{\text{lift}}{qS}$
C_m	pitching moment coefficient, $\frac{\text{pitching moment}}{qS\overline{c}}$
C_n	yawing moment coefficient, $\frac{\text{yawing moment}}{qSb}$
C_Y	side force coefficient, $\frac{\text{side force}}{qS}$
D_m	engine inlet ram drag, N (lb)
i_t	horizontal-tail incidence with respect to horizontal data, positive trailing edge down, deg
M_∞	free-stream Mach number
$\frac{N}{N_d}$	engine speed, fraction of design engine RPM
q_∞	free-stream dynamic pressure, N/sq m (lb/sq ft)
S	wing area, sq m (sq ft)
X_{GW}	gross resultant force of wing jet measured with wind-off, N (lb)
α	aircraft angle of attack referred to the aircraft horizontal data, deg
β	angle of sideslip, deg
δ_a	aileron deflection, (36/24 means left aileron at 36°, right aileron at 24°, positive trailing edge down), deg
$\Delta\delta_a$	differential aileron deflection from nominal value ($\Delta\delta_a$ = 10° means left aileron 10° trailing edge up and right aileron 10° trailing edge down from nominal value), deg
δ_e	elevator deflection, positive trailing edge down, deg

δ_f flap deflection, positive trailing edge down, deg

δ_r rudder deflection, positive trailing edge left, deg

η_{PJ} pitch jet coefficient, positive when blowing directed down, ($|\eta_{PJ}| = 1$ for full blowing up or down)

θ angle of wing jet force measured from horizontal data, deg

Subscripts

a aileron

corr corrected to standard day temperature

f flap

nom nominal

PJ pitch jet

r rudder

u uncorrected

RESULTS OF FULL-SCALE WIND TUNNEL TESTS ON THE H.126 JET FLAP AIRCRAFT

Thomas N. Aiken and Anthony M. Cook

Ames Research Center

SUMMARY

The aerodynamic characteristics of the full-scale H.126 jet flap aircraft were studied in the Ames 40- by 80-Foot Wind Tunnel. The H.126 aircraft is designed for research on flight characteristics of an aircraft using the jet flap principle.

Static longitudinal, lateral, and directional characteristics were measured at a Reynolds number of 2.5 to 2.7 million. The jet control power as well as the aerodynamic characteristics were measured and are presented herein with limited discussion. The primary configuration variables were flap and aileron deflection.

INTRODUCTION

The Hunting H.126 aircraft was built to study the jet flap principle in flight. It has been extensively flight tested although the data from these tests are as yet unpublished. Several small-scale wind tunnel tests have also been made on this and similar configurations (ref. 1). A brief history of the aircraft is presented in reference 2.

This report presents the results of low-speed tests on the full-scale research aircraft in the Ames 40- by 80-Foot Wind Tunnel. The purposes of the tests were to evaluate the longitudinal and lateral-directional characteristics of the aircraft in high lift configurations and to provide data for correlation with small-scale wind-tunnel and flight-test results.

The aircraft was tested out of ground effect with flap settings of 0°, 30°, and 40° at various jet momentum coefficients, and with the ailerons symmetrically deflected to 0°, two-thirds, or 100 percent of the flap deflection. The investigation also included the effects of differential aileron deflection and tail incidence.

MODEL AND APPARATUS

Figure 1 shows the aircraft mounted in the wind tunnel. Table 1 presents the basic geometric data of the aircraft. Sketches of the geometry are shown in figure 2.

The blowing systems are shown schematically in figure 3. A portion of the exhaust gas from the engine is blown through full span coverging nozzles and over the flap and aileron upper surfaces to provide the jet sheet. The remainder of the exhaust gas is ducted to two thruster nozzles and the control reaction jets. The distribution of the total mass flow from the engines to the jet flap, the thruster nozzles, and the control jets, when fully open, is 55, 30, and 15 percent, respectively.

The pitch and yaw control jets each received 5 percent while the two roll jets each received 2.5 percent of the mass flow when fully open. The pitch jets were geared to the horizontal tail as shown in figure 4 and operated throughout the test. The yaw jets were locked in an open, neutral position throughout the test. During most of the tests, the roll jets were closed. For one run, however, the roll jets were fully open in the direction of positive roll.

The elevator and horizontal stabilizer were geared together to operate as shown in figure 4. The flaps and ailerons were geared to move together, acting as a single full span flap. The gearing ratio could be adjusted to provide symmetrical aileron deflections of zero, two-thirds, or 100 percent of the flap deflection for any flap angle. Differential aileron settings were possible at all nominal aileron settings.

TESTS

Table 2 provides a convenient index to all the test parameters. All tests were made with the horizontal tail installed.

The tests were conducted at two values of dynamic pressure and several aircraft power settings to obtain a C_J range from 0 to 0.87. Nominal free-stream dynamic pressures used were 350 (7.3) and 407 (8.5) N/sq m (lb/sq ft) giving unit Reynolds numbers of 0.50 and 0.54 million per foot. Most runs were made by varying angles of attack at constant sideslip or varying sideslip at constant angle of attack. Among the test parameters were jet momentum coefficient, flap angle, tail incidence, differential aileron angle, and rudder angle. Static tests were also made to evaluate the wing jet force.

DATA REDUCTION

The moment center used in the data reduction was located at $0.40\,\bar{c}$ on the aircraft horizontal data. The forces were resolved with respect to the wind axes, while the moments were resolved with respect to the stability axes. The engine inlet ram drag has not been removed from the data.

The wing jet momentum force, X_{GW}, was obtained from measurements of the total static force from wind-off tests. The wing force was separated from the total airplane static force by using relationships given in the aircraft operations manual. These relationships assert that the thrusters contribute 0.6 X_{GW} to axial thrust and that the pitch jets contribute 0.1 (η_{PJ}) (X_{GW}) to lift. Using the following equations for the lift and thrust components of the total force and the above relations, the jet angle, θ, and X_{GW} may be found by an interation process:

$$\text{Lift} = X_{GW} \sin\theta + 0.1(\eta_{PJ})(X_{GW})$$
$$\text{Thrust} = X_{GW} \cos\theta + 0.6\, X_{GW}$$

The static values of X_{GW} so obtained are compared in figure 5 with those given in the operations manual. The engine inlet ram drag and the C_J values are also given in figure 5. The engine inlet ram drag and X_{GW} have been corrected to standard day conditions. The jet angle, θ, was found to be approximately 25° greater than the geometric flap angle, δ_f. Based on measurements of duct pressures taken during the static tests, the pitch jet and roll jet forces were found to be approximately 8 and 4 percent, respectively, of the wing jet force.

Due to the uncertainties of determining wind-tunnel wall corrections of models with powered lift components and high downwash angles the data presented here have not been corrected for tunnel wall effects. However, the effect of standard wall corrections on representative data are shown in figure 6. The wind-tunnel wall corrections used in figure 6 were based on the "aerodynamic or circulation C_L" computed as follows:

$$C_{L_{aero}} = C_L - C_J \sin(\alpha + \theta) - 0.6\, C_J \sin\alpha$$

Based on this relationship and the standard 40- by 80-foot wind tunnel corrections, the corrected coefficients are:

$$C_D = C_{D_u} + 0.00754\, C_{L_{aero}}^2$$
$$\alpha = \alpha_u + 0.437\, C_{L_{aero}}$$
$$C_m = C_{m_u} + 0.0233\, C_{L_{aero}}$$

RESULTS

The basic-wind tunnel data are presented graphically in figures 7 to 17. Table 2 is an index to the data figures and major independent test parameters. No wind-tunnel wall corrections have been applied to these data. The values of C_J listed in the figures were computed from the X_{GW} in figure 5 and based on the nominal dynamic pressure during the run. All angle-of-attack polars were done at zero yaw angle unless otherwise noted. Arrows on roll data indicate direction of off-scale data.

DISCUSSION

The longitudinal characteristics shown in figure 7 indicate the aircraft has static longitudinal stability up to stall. The stall occurs with no pitch-up, but lift drops very abruptly with one wing stalling before the other. The data also indicate that increasing symmetric aileron deflection increases the lift at a given C_J and α.

Figure 8 indicates a reduction in stall angle of attack, and an increase in drag and moment change after stall when the aircraft is yawed. However, as shown in figure 9, asymmetric aileron defection has no appreciable effect on these characteristics.

The effect of stall on the lateral-directional characteristics is shown in figure 11. As noted previously, one wing stalls before the other, separated by as much as 5° in angle of attack. This causes large roll and yawing moments after stall. It was evident that either wing could stall first, there being no discernible preferred direction. Tuft studies indicated that the separation started at the midchord of either wing and spread over the entire wing within 2° increase of incidence. The flow over the leading edge and flap remained attached.

It should not be deduced from these facts that all jet flap aircraft will have these adverse stalling characteristics. The H.126 wing is a slightly tapered, twisted thick, straight wing. As such, it is uniformly loaded and stalls simultaneously over the entire wing. A jet flap with greater taper and sweep, and a thinner wing section will stall more gradually because of the nonuniform loading.

Figures 11(c), 13, and 14 indicate the ailerons provide insufficient roll power to control the asymmetric stall. The data also indicate that increasing symmetric aileron deflection reduces the roll power available using asymmetric aileron deflection. Asymmetric aileron deflection produced adverse yaw as shown in figure 14.

A comparison of figures 14(a), 14(b), and 17 indicate that application of power to the roll jets increases the roll power available. However, for the test configurations represented, the increase from the unpowered configuration decreases as more aileron deflection is used indicating an adverse interference on the aileron.

Ames Research Center
National Aeronautics and Space Administration
Moffett Field, Calif., Oct. 30, 1972

REFERENCES

1. Butler, S. F. J.; Guyett, M. B.; and Moy, B. A.: Six-Component Low-Speed Tunnel Tests of Jet-Flap Complete Models with Variation of Aspect Ratio, Dihedral, and Sweepback, Including the Influence of Ground Proximity. R.A.E. Rep. Aero 2652, June 1961.

2. Harris, K. D.: The Hunting H.126 Jet-flap Research Aircraft. AGARD Lecture Series 43, February, 1971.

TABLE 1.– H.126 GEOMETRIC DATA

Wing	
Airfoil section	NACA 4424
Area, sq m (sq ft)	20.51 (220.95)
Aspect ratio	9.32
Mean aerodynamic chord, $\bar{c}$, m (ft)	1.54 (5.05)
Span, m (ft)	13.83 (45.37)
Sweep, 0.25 chord, deg	5.03
Dihedral, deg	4
Root chord, m (ft)	1.96 (6.42)
Tip chord, m (ft)	1.01 (3.31)
Incidence (to aircraft data), deg	5
Taper ratio	0.516
Flap and aileron	
Flap inboard edge semispan position	0.13
Flap proportion of semispan	0.41
Flap root chord, m (ft)	0.39 (1.27)
Flap tip chord, m (ft)	0.30 (1.00)
Aileron inboard edge semispan position	0.54
Aileron proportion of semispan	0.41
Aileron root chord, m (ft)	0.30 (0.99)
Aileron tip chord, m (ft)	0.22 (0.72)
Horizontal tail	
Airfoil section (inverted)	NACA 43015
Area, sq m (sq ft)	5.11 (55.00)
Elevator area (aft of hinge), sq m (sq ft)	1.46 (15.75)
Aspect ratio	2.55
Span, m (ft)	3.61 (11.83)
Root chord, m (ft)	2.12 (6.96)
Tip chord, m (ft)	0.71 (2.32)
Taper ratio	0.33
Elevator root chord, m (ft)	0.53 (1.74)
Elevator tip chord, m (ft)	0.28 (0.93)
Horizontal tail volume	1.16
Vertical tail	
Airfoil section	NACA 0015
Area (above fuselage), sq m (sq ft)	4.93 (53.00)
Rudder area (aft of hinge), sq m (sq ft)	0.86 (9.30)
Aspect ratio	1.17
Vertical tail height, m (ft)	2.41 (7.90)
Root chord m (ft)	2.54 (8.33)
Tip chord, m (ft)	1.55 (5.08)
Rudder height, m (ft)	1.46 (4.80)
Rudder root chord, m (ft)	0.67 (2.21)
Rudder tip chord, m (ft)	0.51 (1.67)

TABLE 1.– H.126 GEOMETRIC DATA – Concluded

Fuselage	
Height (including canopy), m (ft)	2.57 (8.44)
Width, m (ft)	1.27 (4.16)
Length, m (ft)	13.43 (44.08)
Thrust nozzles and reaction jets	
Thrust; below moment center, m (ft)	0.95 (3.10)
behind moment center, m (ft)	1.96 (6.42)
Moment arm of reaction jets about moment center;	
pitch, m (ft)	8.19 (26.85)
roll, m (ft)	6.74 (22.1)
yaw, m (ft)	5.92 (19.42)

TABLE 2.– DATA INDEX

TABLE 2.– DATA INDEX – Concluded

		Figure
D.	Asymmetric δ_a (vs $\Delta\delta_a$);	
	$\delta_f = 40°$, $\delta_{a_{nom}} = 40/40$, $\alpha = 0°$	14(a)
	$\alpha = 10°$	(b)
	$\delta_{a_{nom}} = 26/26$, $\alpha = 0°$	(c)
	$\alpha = 10°$	(d)
	$\delta_{a_{nom}} = 0/0$, $\alpha = 0°$	(e)
	$\alpha = 10°$	(f)
	$\delta_f = 30°$, $\delta_{a_{nom}} = 30/30$, $\alpha = 0°$	(g)
	$\alpha = 10°$	(h)
E.	Sideslip, β;	
	$\delta_f = 40°$, $\delta_a = 40/40$, $\alpha = 0°$	15(a)
	$\alpha = 10°$	(b)
	$\delta_f = 30°$, $\delta_a = 30/30$, $\alpha = 0°$	(c)
	$\alpha = 8°, 10°$	(d)
F.	Rudder deflection;	
	$\delta_f = 40°$, $\delta_a = 0/0$, $C_J = 0.43$	16(a)
	$C_J = 0.63$	(b)
	$C_J = 0.87$	(c)
G.	Roll jets;	
	$\delta_f = 40°$, $\delta_a = 40/40$ (jet full right roll)	17

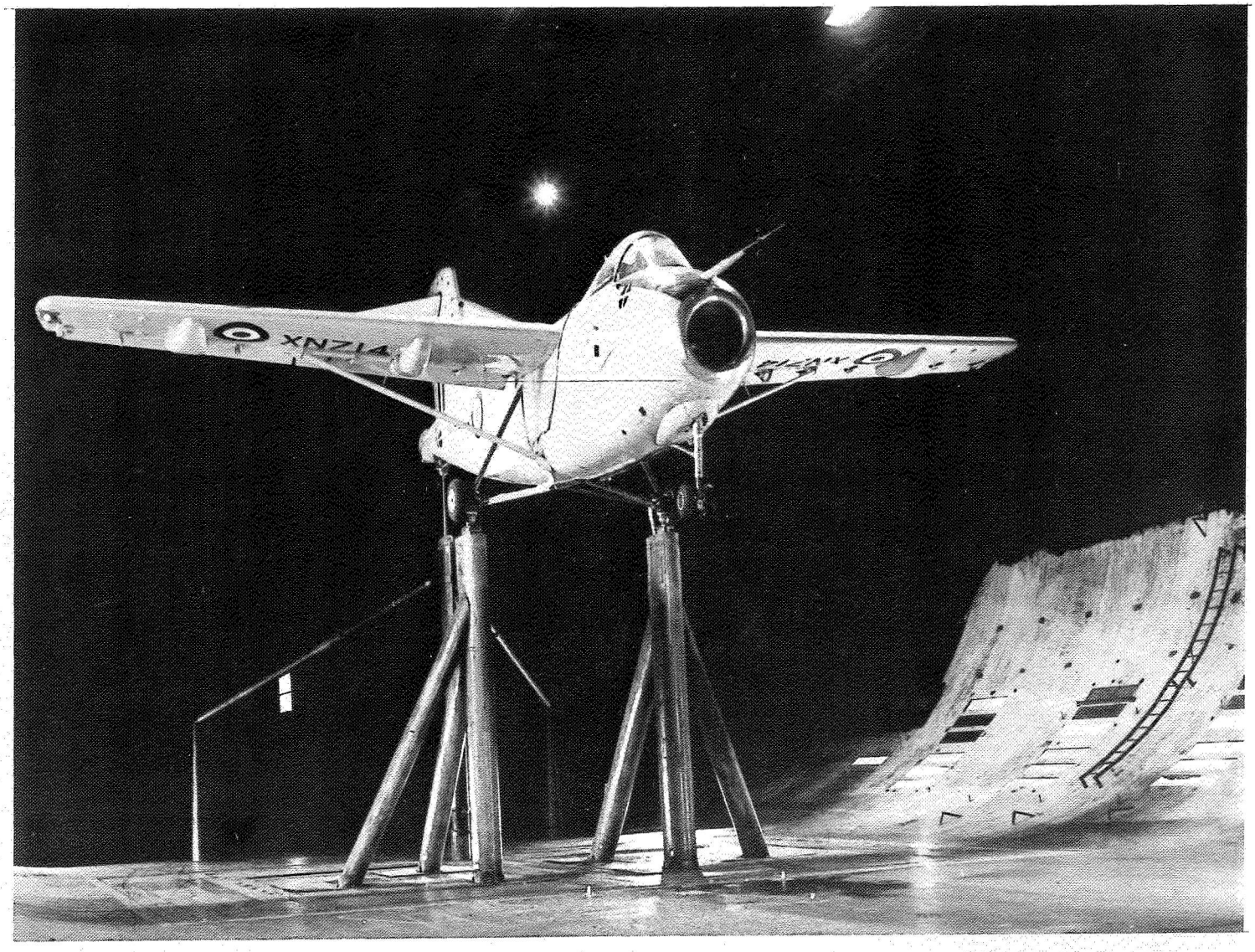

(a) Three-quarter front view.

Figure 1.– Aircraft installed in the Ames 40– by 80–Foot Wind Tunnel.

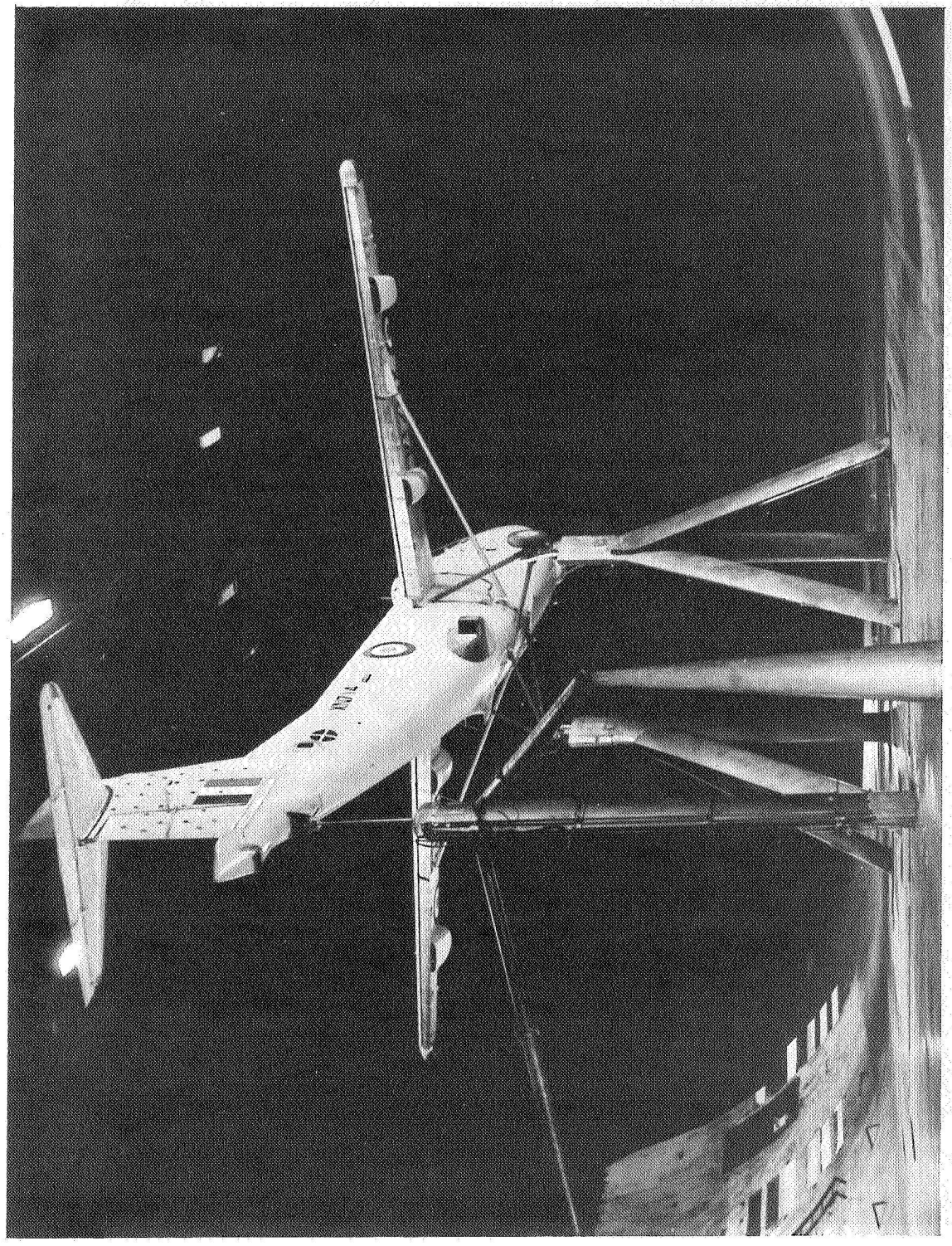

(b) Three-quarter rear view.

Figure 1.– Concluded.

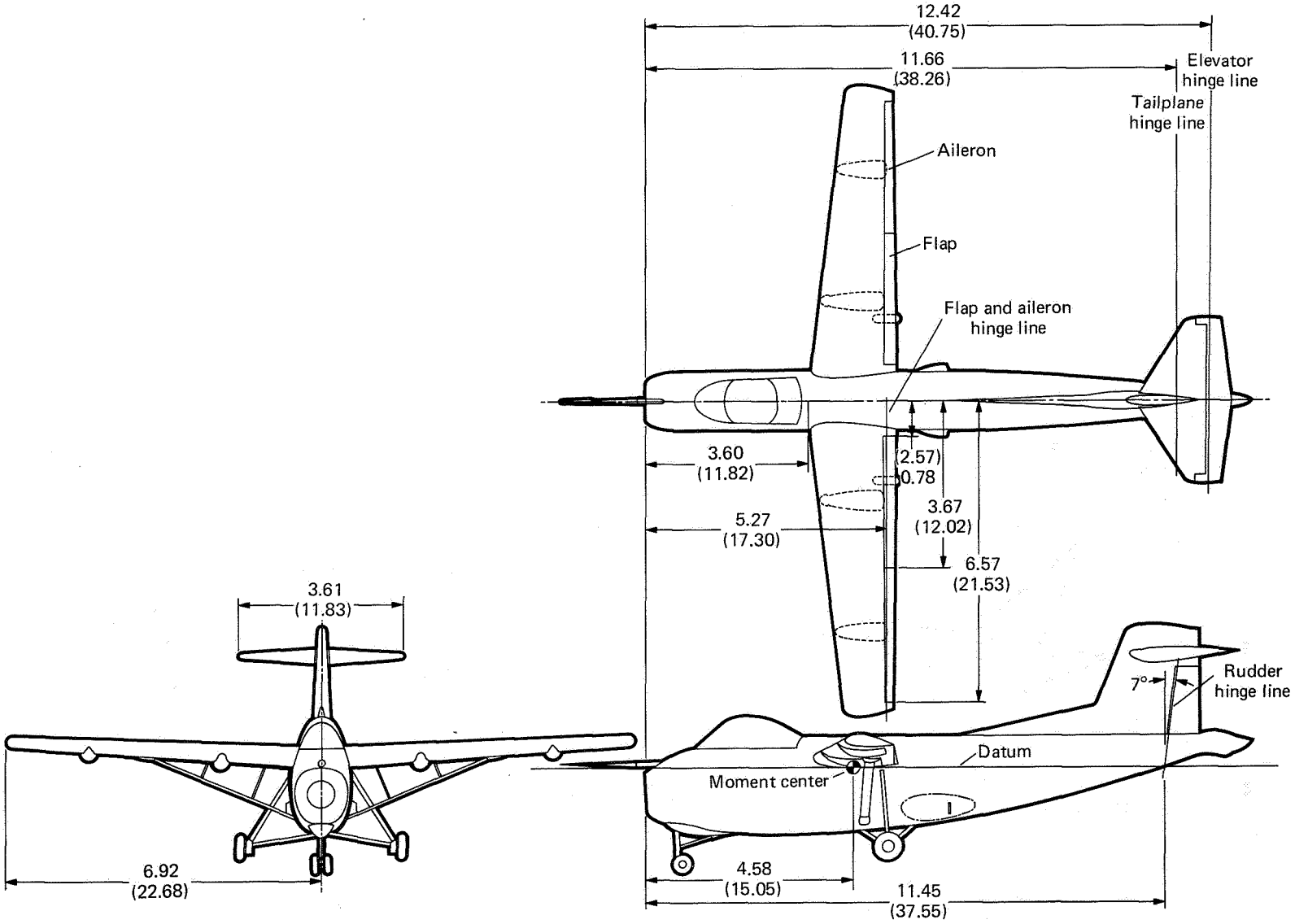

(a) Three-view drawing of the aircraft, dimensions in meters (feet).

Figure 2.– Geometric details of the aircraft.

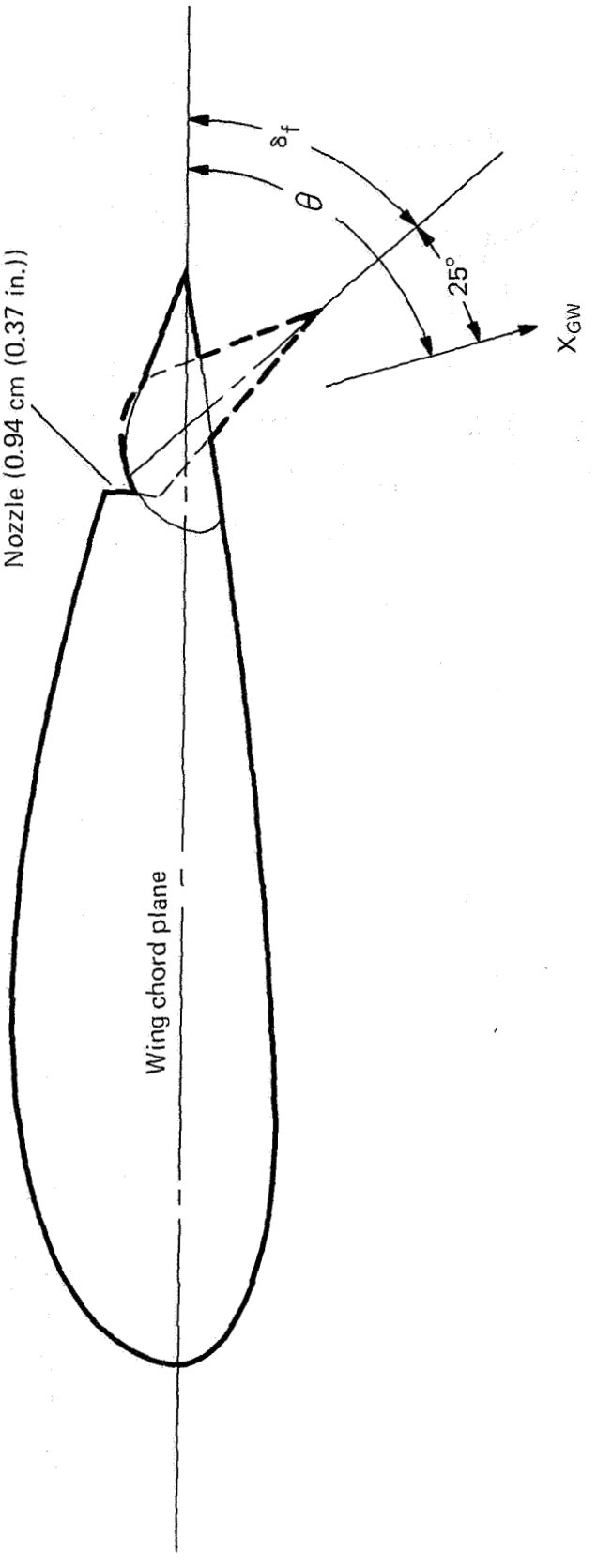

(b) Typical wing section geometry through flap or aileron.

Figure 2.– Continued.

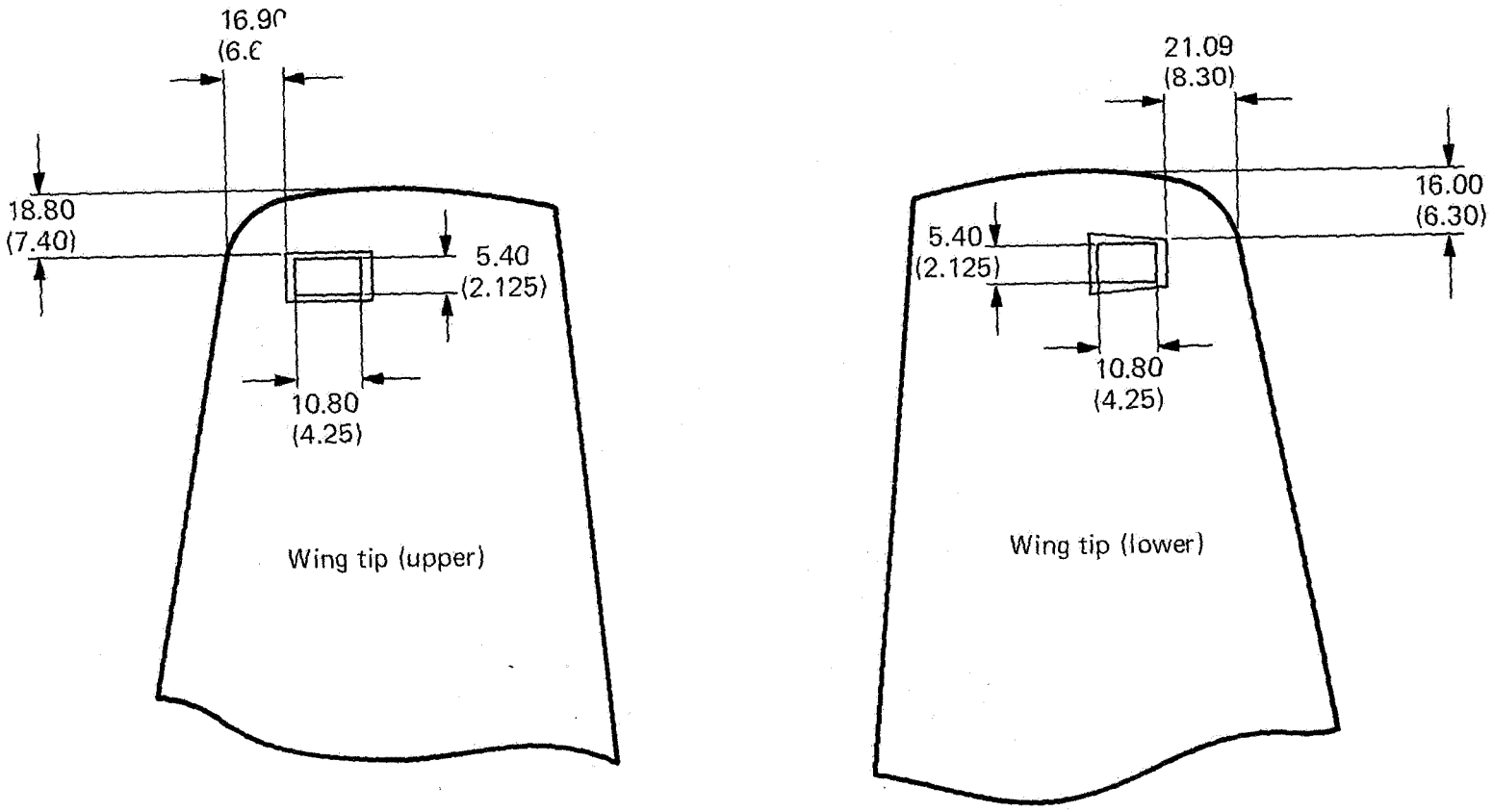

(c) Schematic of roll jets, dimensions in cm (in).

Figure 2.– Concluded

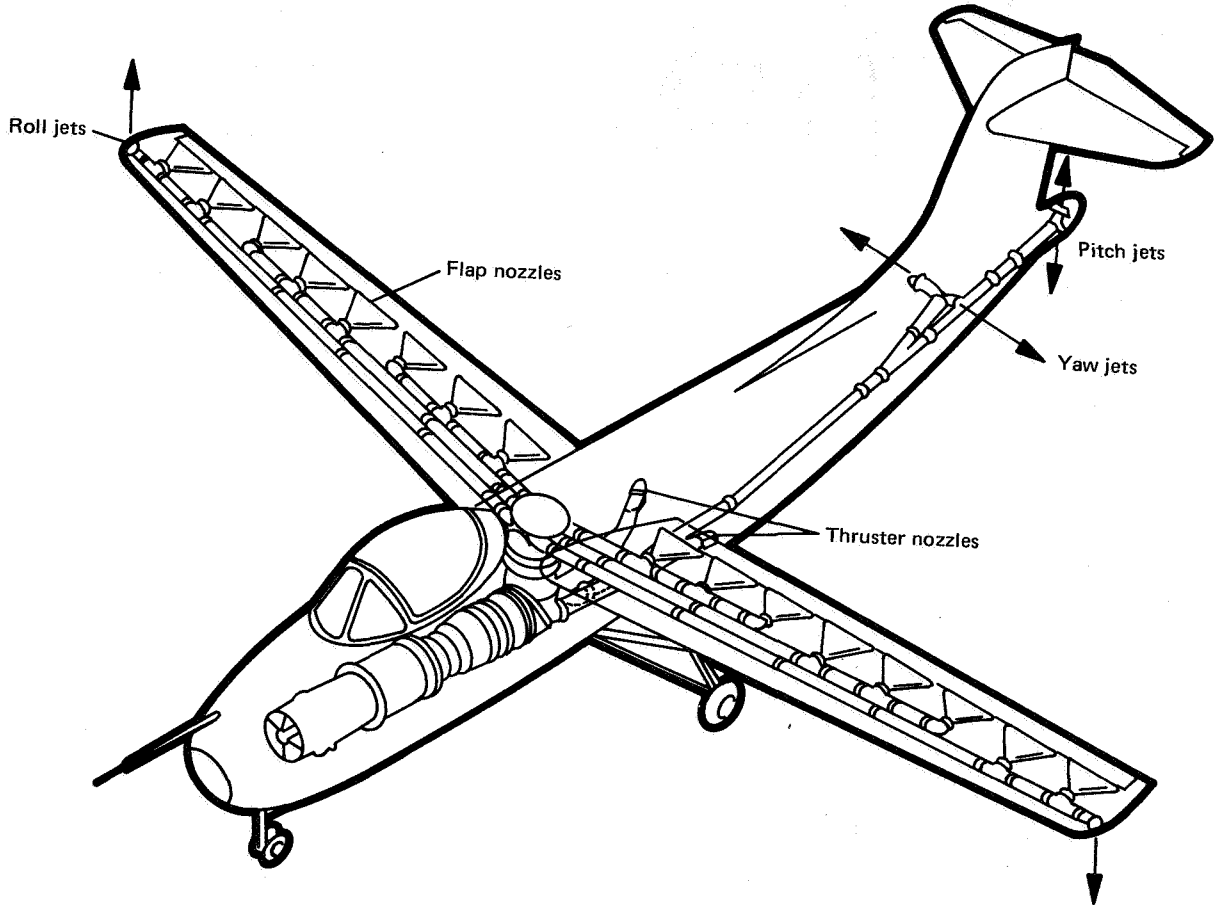

Figure 3.– Schematic of H.126 blowing systems.

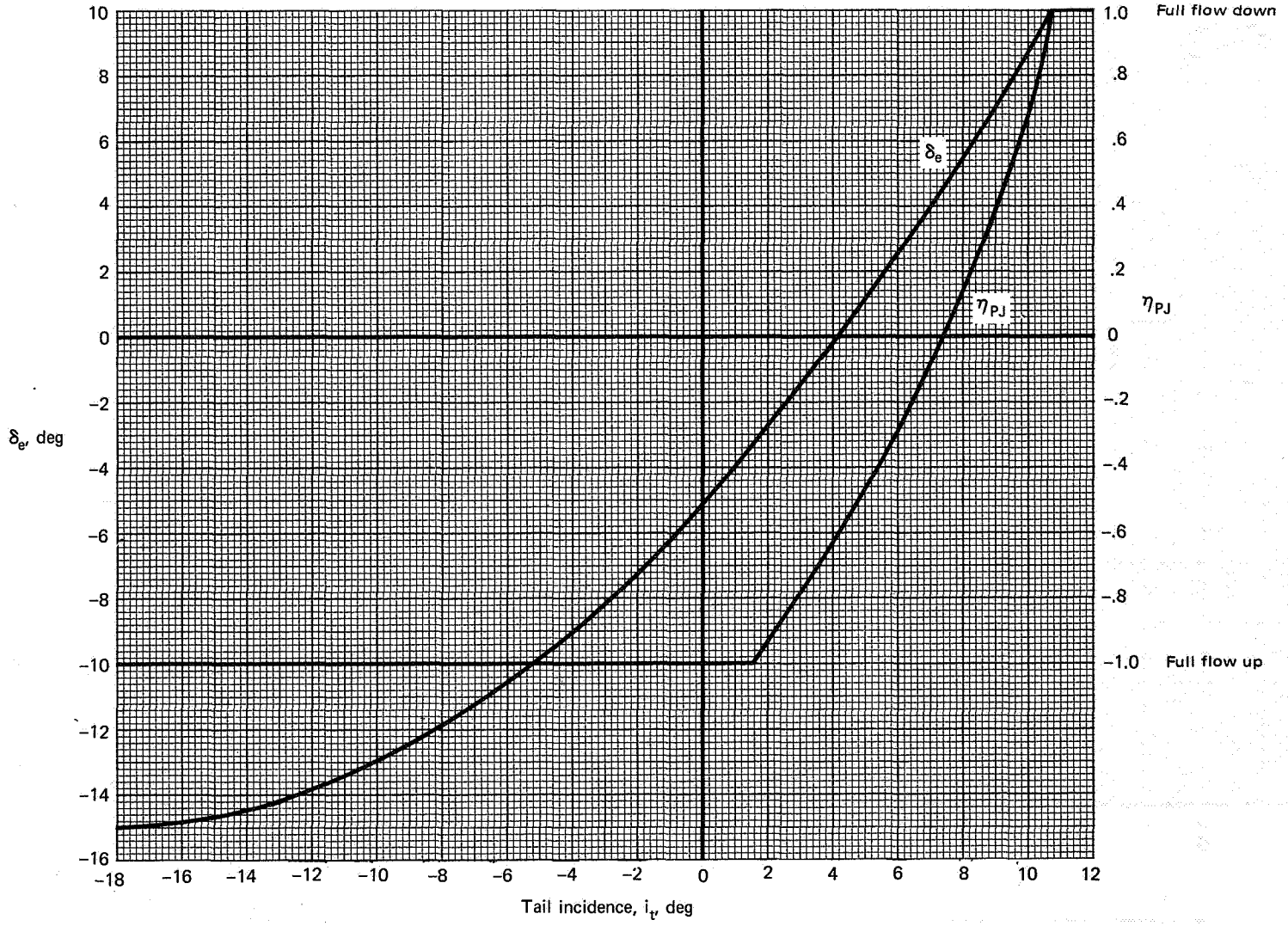

Figure 4.– Horizontal-tail incidence, pitch jet, and elevator gearing.

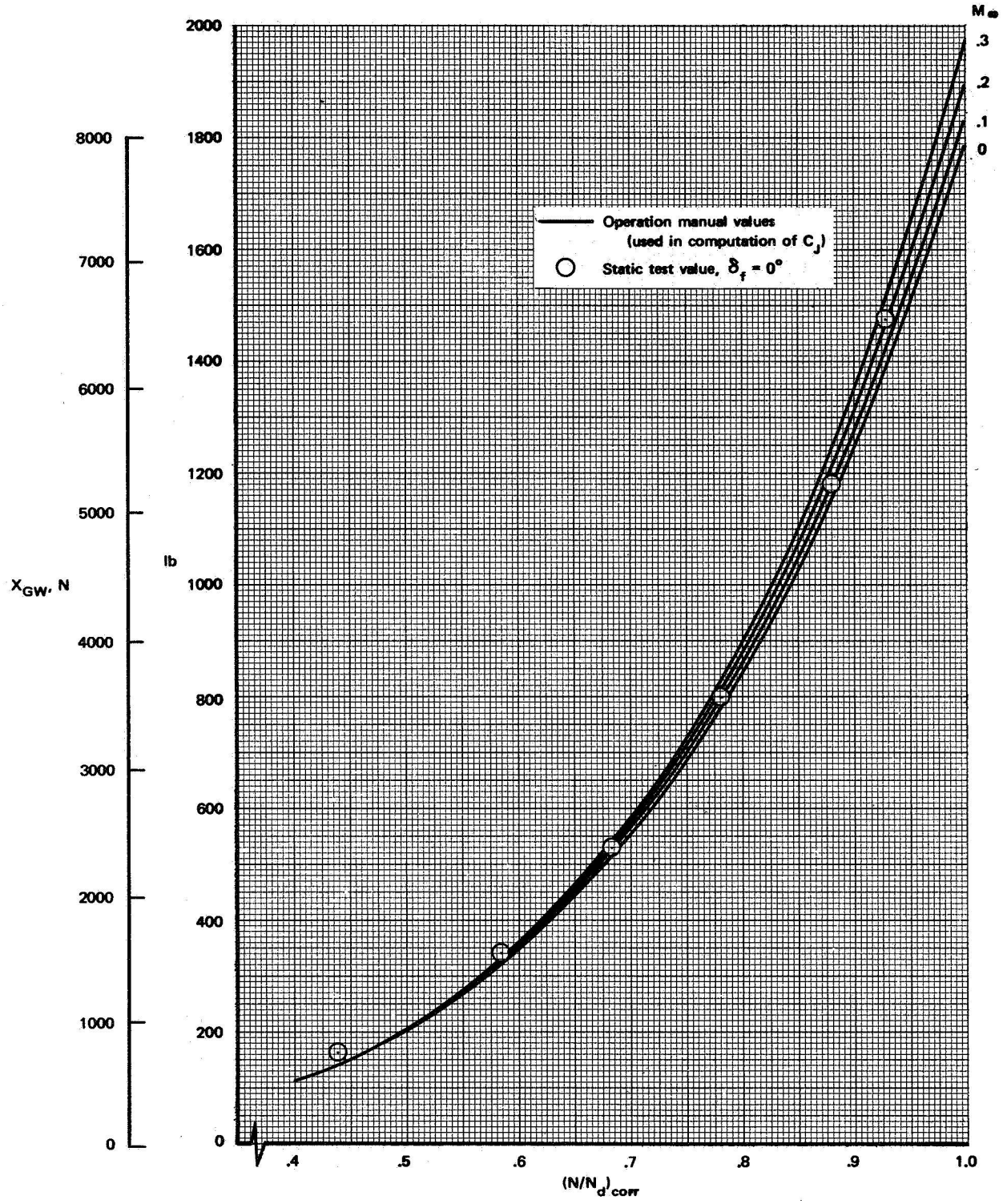

(a) Wing jet force vs engine speed, corrected to standard day.

Figure 5.– Propulsive characteristics of the H.126 aircraft.

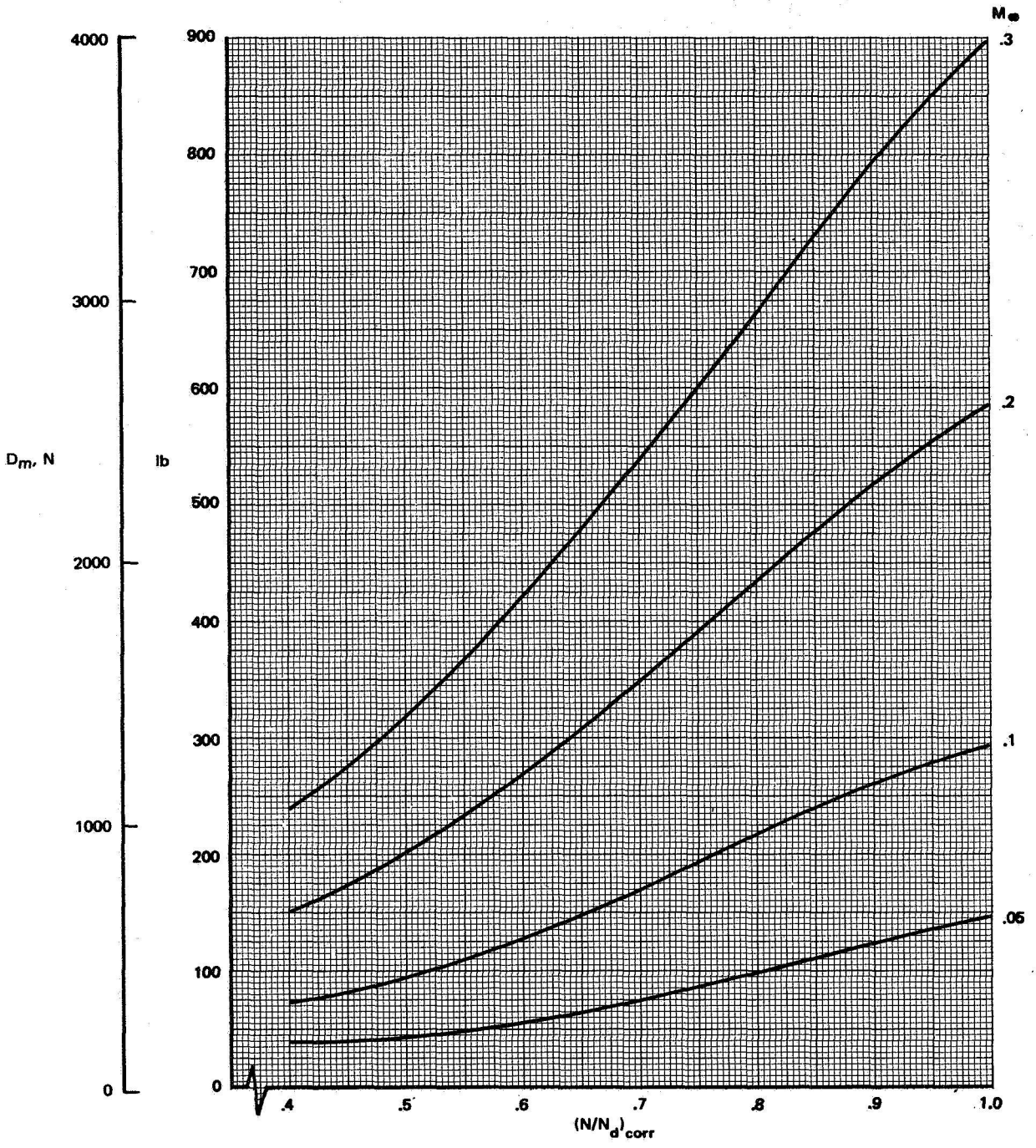

(b) Engine inlet ram drag vs engine speed, standard day.

Figure 5.– Continued.

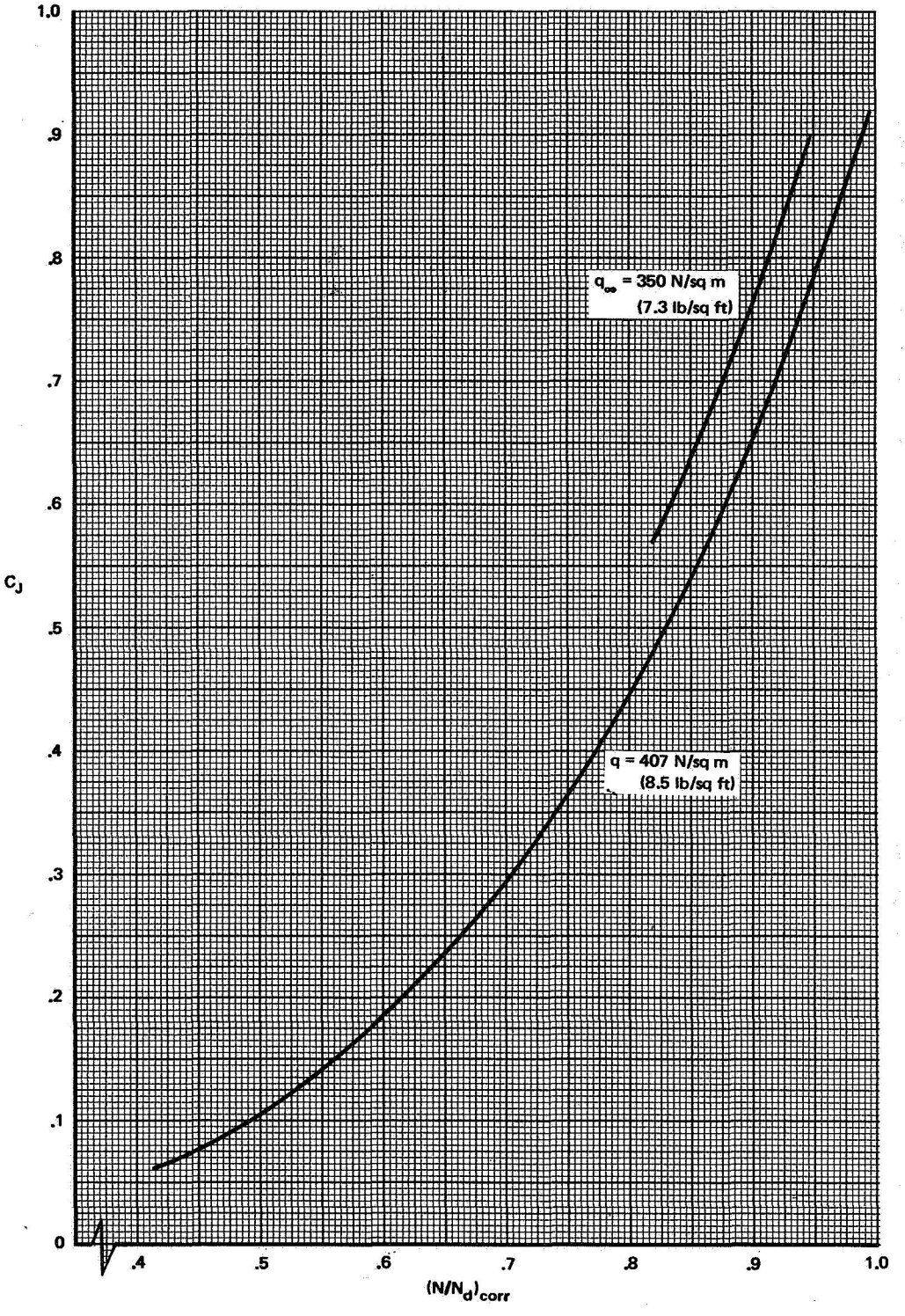

(c) Jet momentum coefficient vs engine speed.

Figure 5. – Concluded.

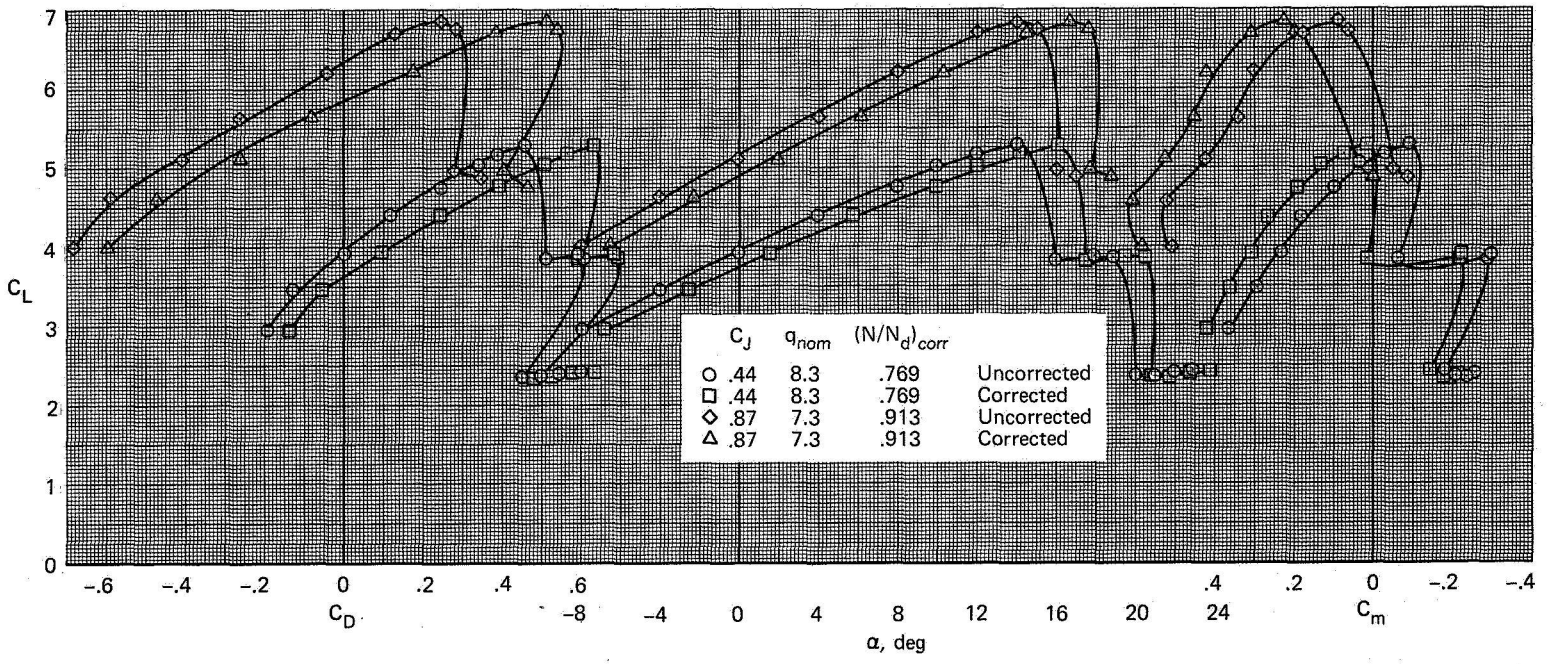

Figure 6.– Effect of wind tunnel wall corrections applied to the data of figure 7(b); $\delta_f = 40$, $\delta_a = 40/40$, $i_t = 4$.

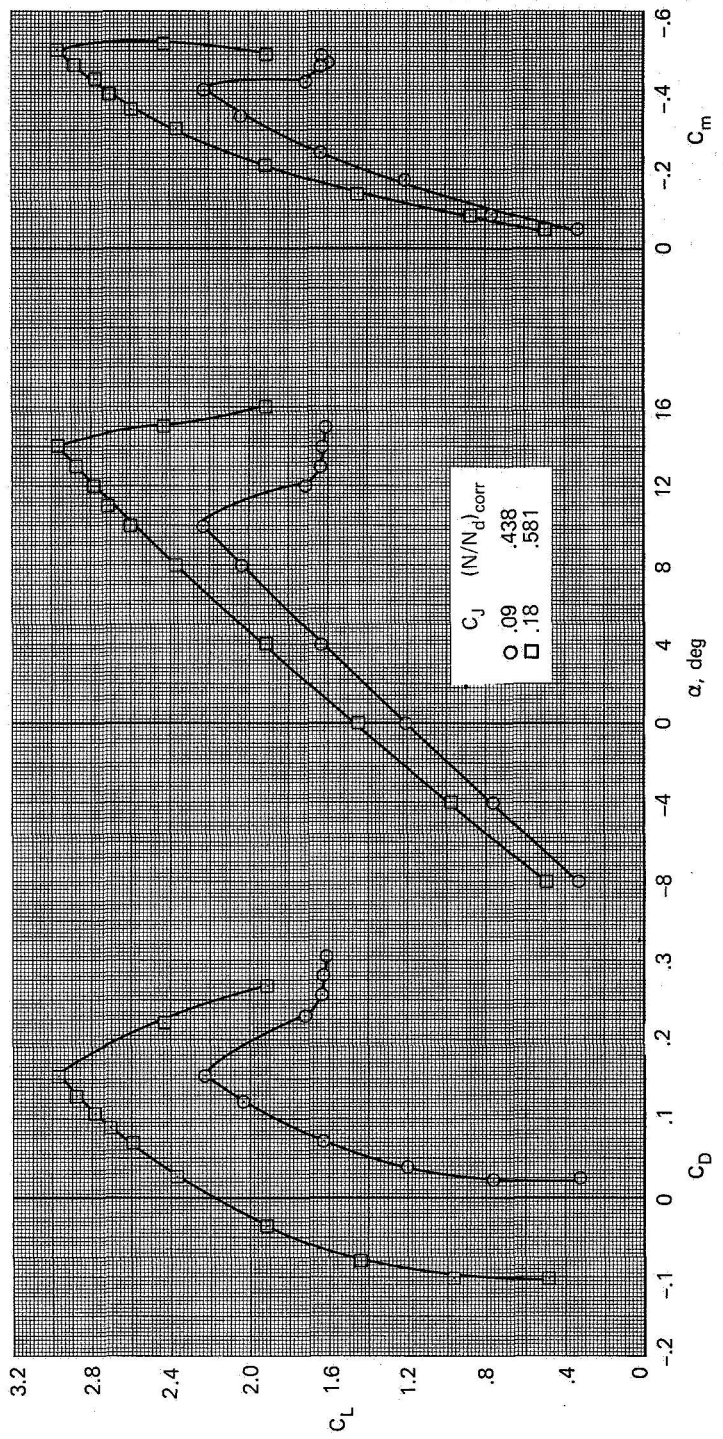

(a) $\delta_f = 0, \delta_a = 0/0, i_t = 7, q_{nom} = 8.6$

Figure 7.– The effect of C_J on the longitudinal characteristics of the aircraft.

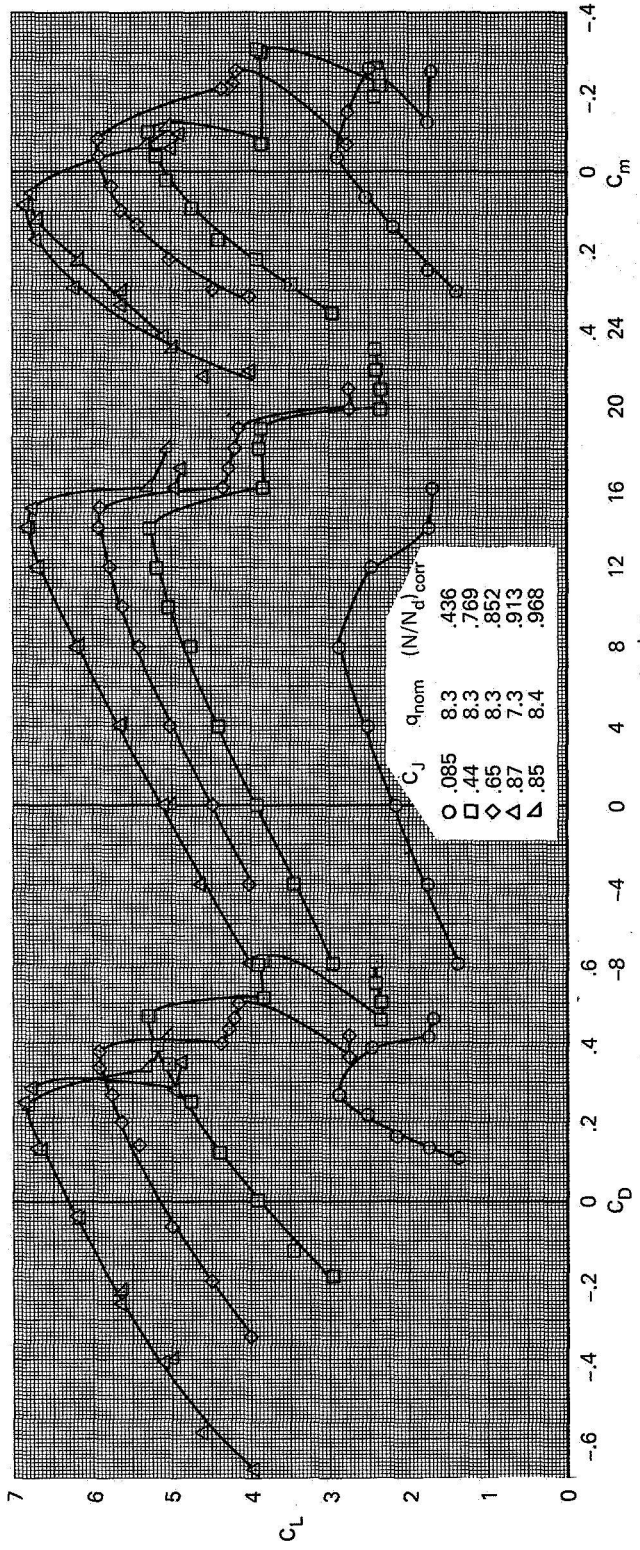

(b) $\delta_f = 40, \delta_a = 40/40, i_t = 4$

Figure 7.– Continued.

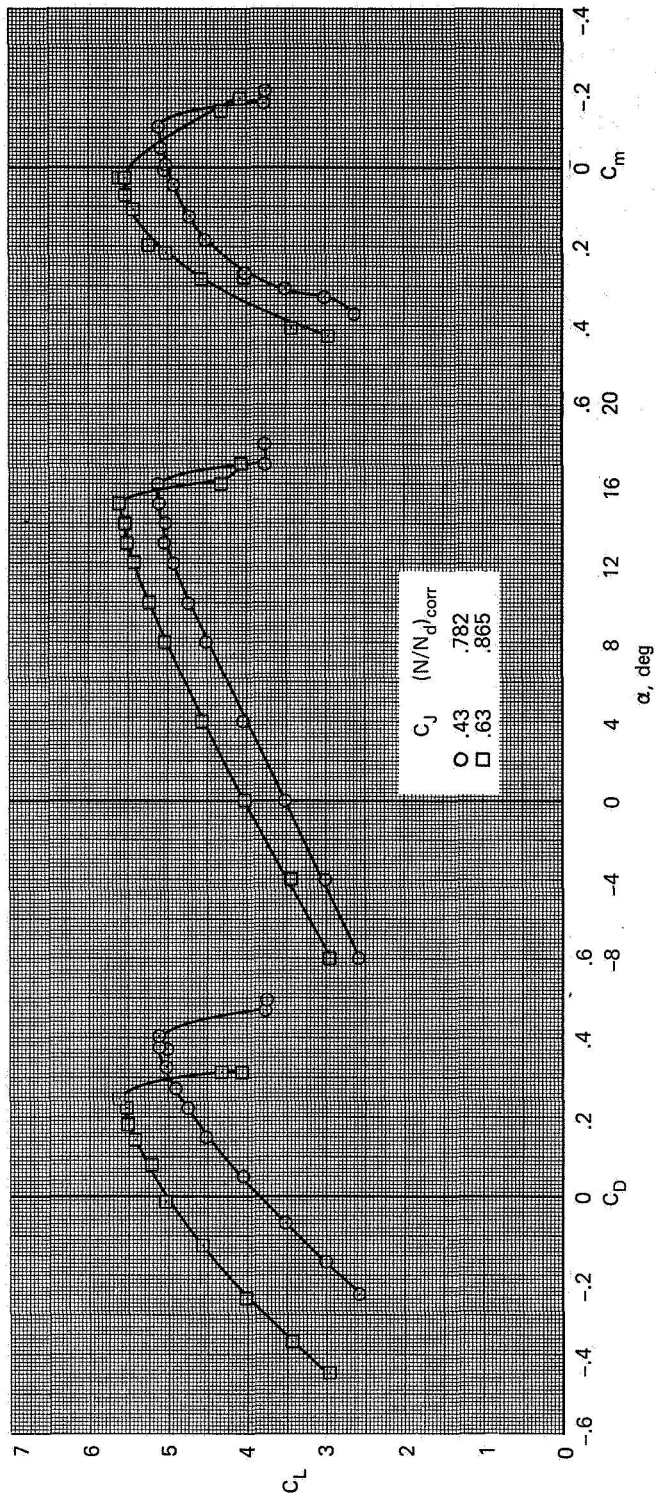

(c) $\delta_f = 40, \delta_a = 26/26, i_t = 4, q_{nom} = 8.5$

Figure 7.– Continued.

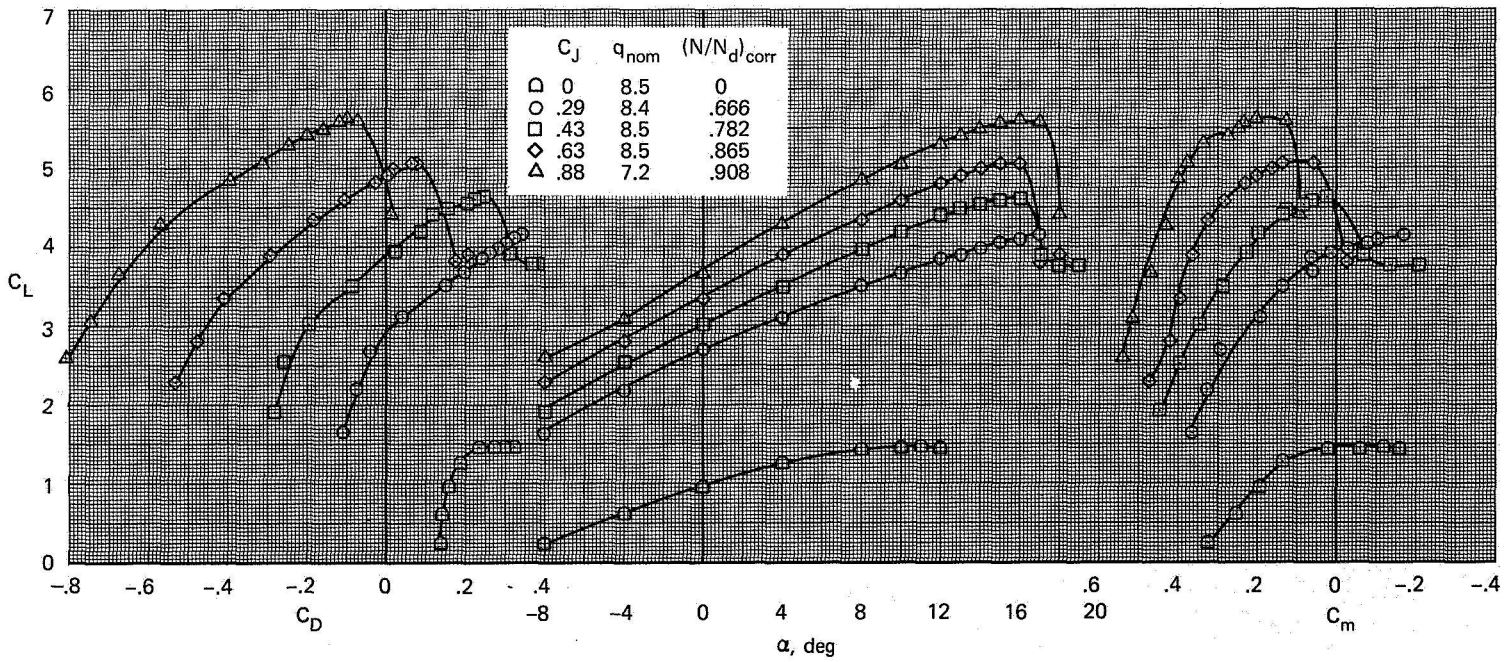

(d) $\delta_f = 40, \delta_a = 0/0, i_t = 4$

Figure 7.– Continued.

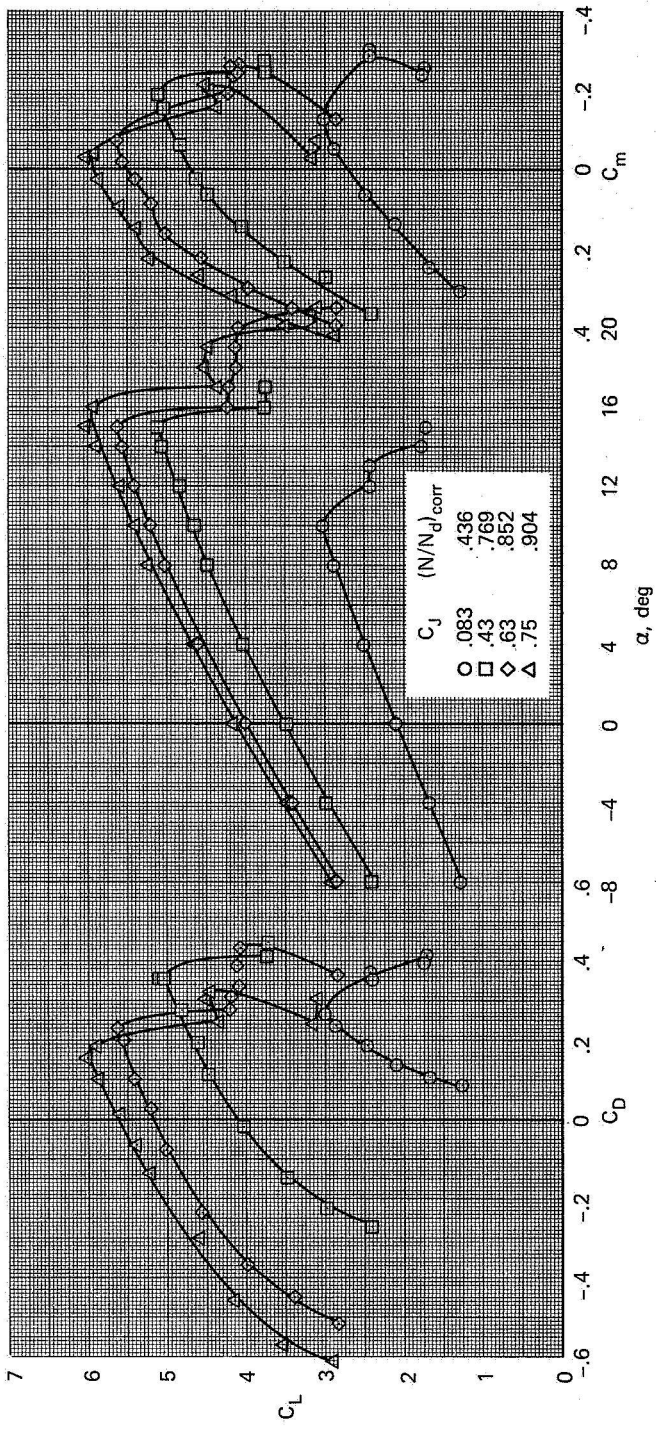

(e) $\delta_f = 30, \delta_a = 30/30, i_t = 4, q_{nom} = 8.5$

Figure 7.– Concluded.

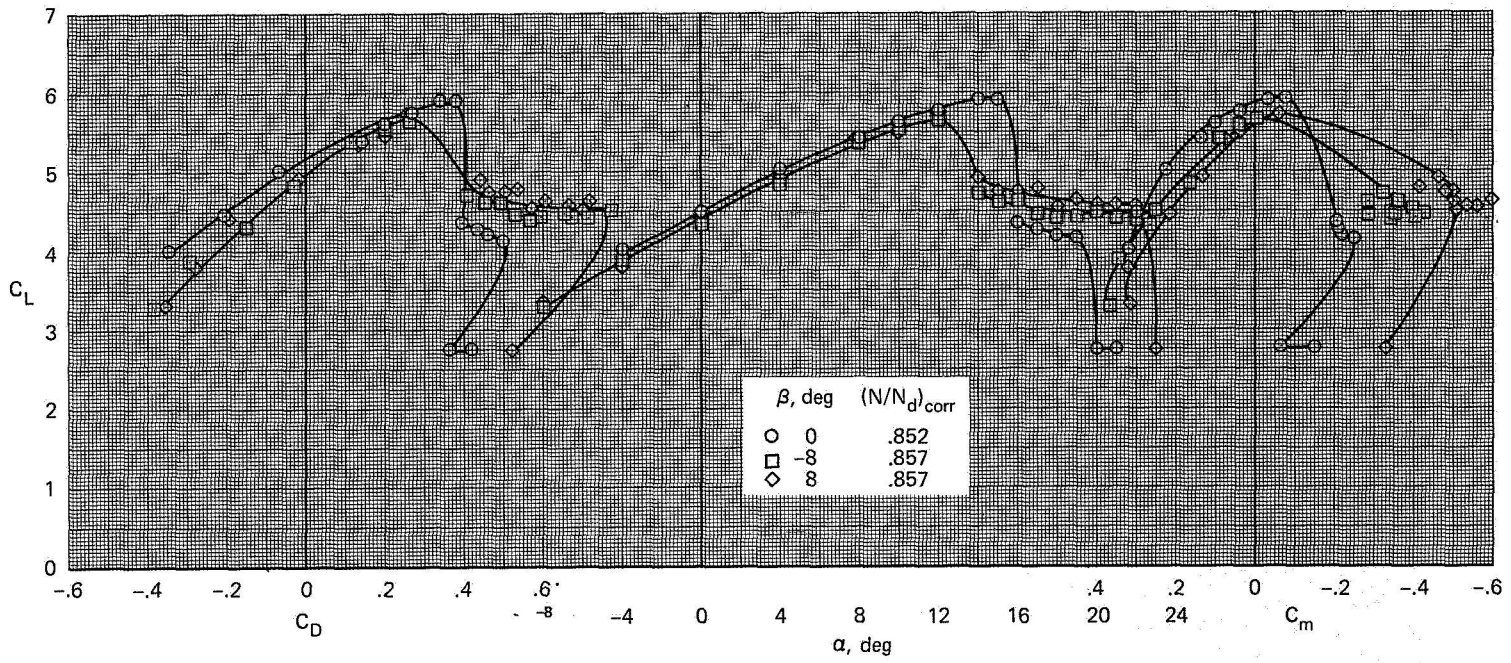

Figure 8.– The effect of sideslip on the longitudinal characteristics of the aircraft; $\delta_f = 40$, $\delta_a = 40/40$, $i_t = 4$, $C_J = 0.65$, $q_{nom} = 8.3$.

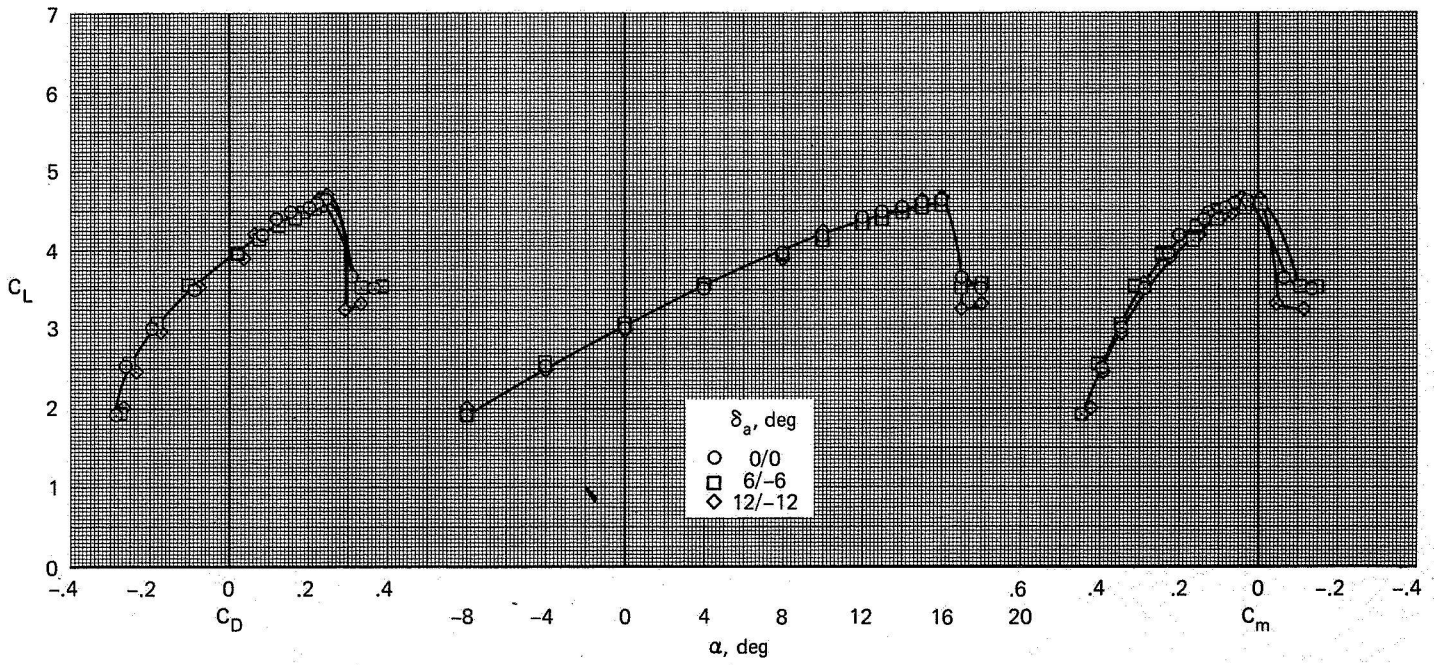

(a) $\delta_{a_{nom}} = 0/0$, $(N/Nd)_{corr} = 0.782$

Figure 9.– The effect of asymmetric aileron deflection on the longitudinal characteristics of the aircraft; $\delta_f = 40$, $i_t = 4$, $C_J = 0.43$, $q_{nom} = 8.5$.

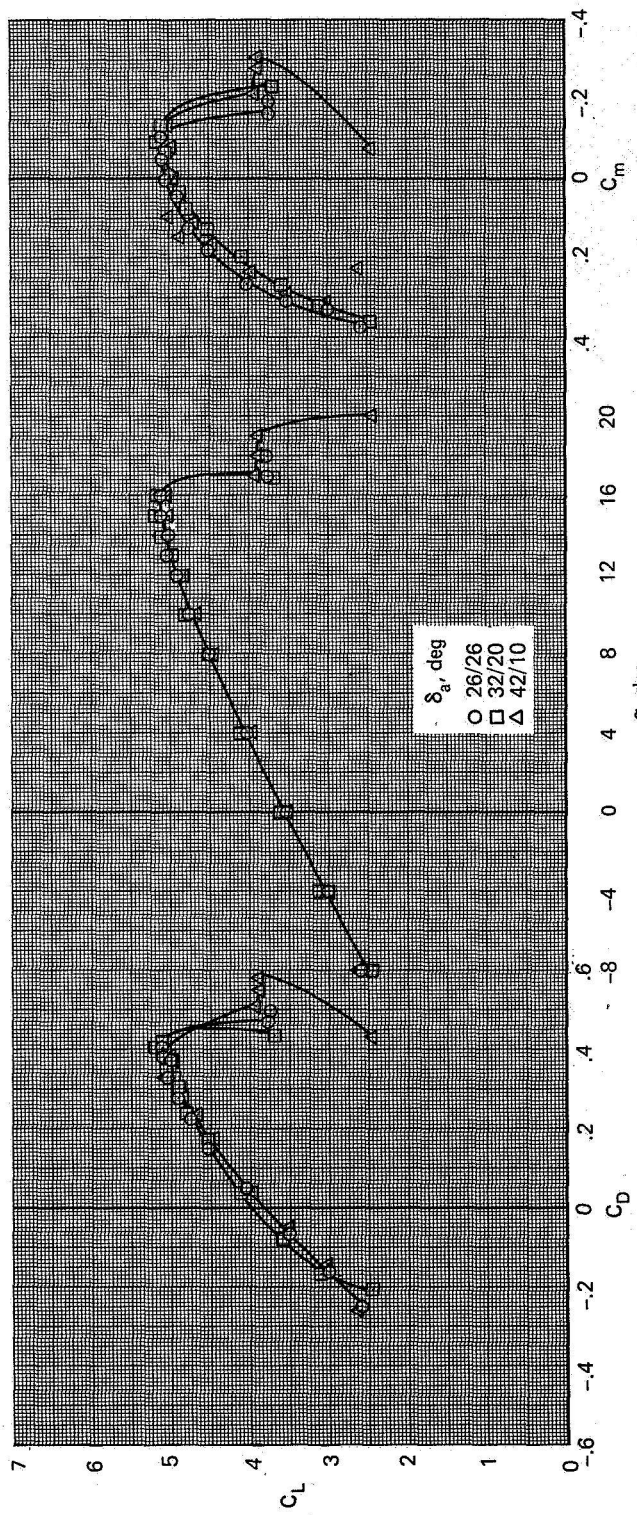

(b) δa_{nom} = 26/26, $(N/Nd)_{corr}$ = 0.782

Figure 9.– Continued.

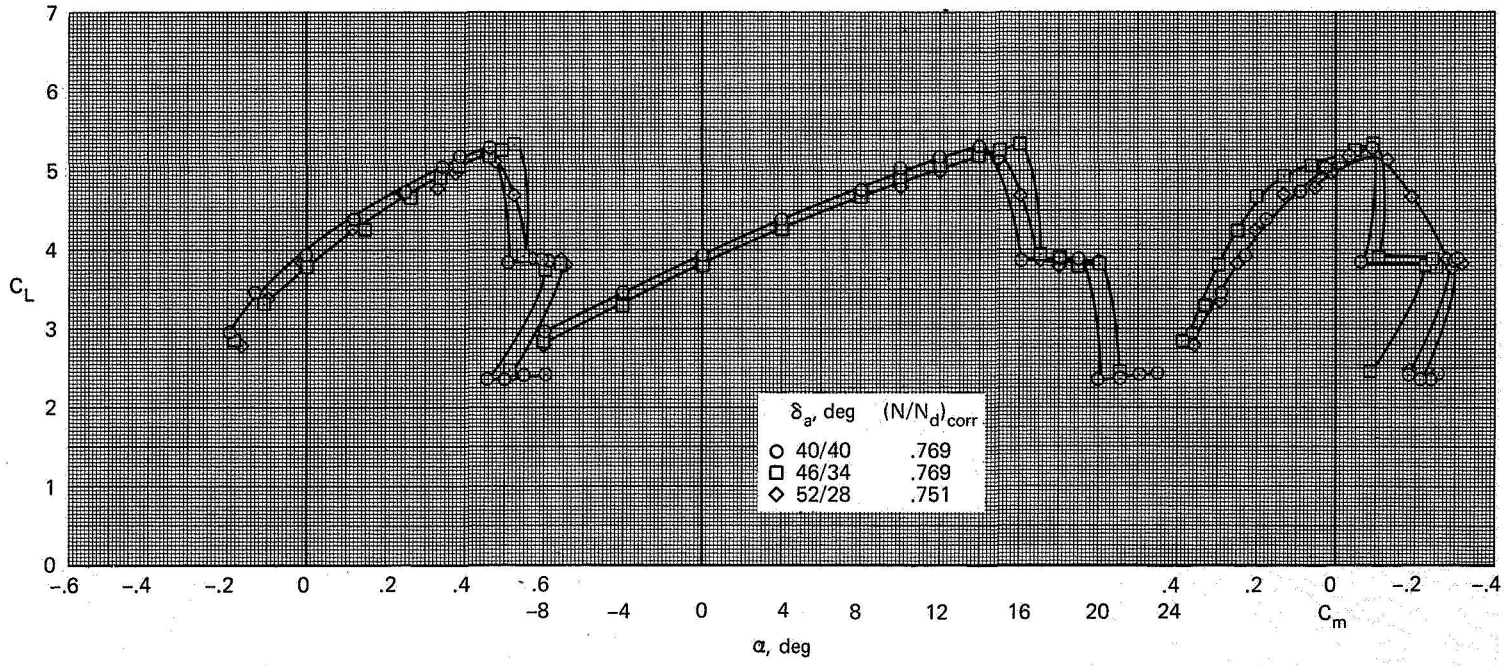

(c) $\delta_{a_{nom}} = 40/40$

Figure 9.– Concluded.

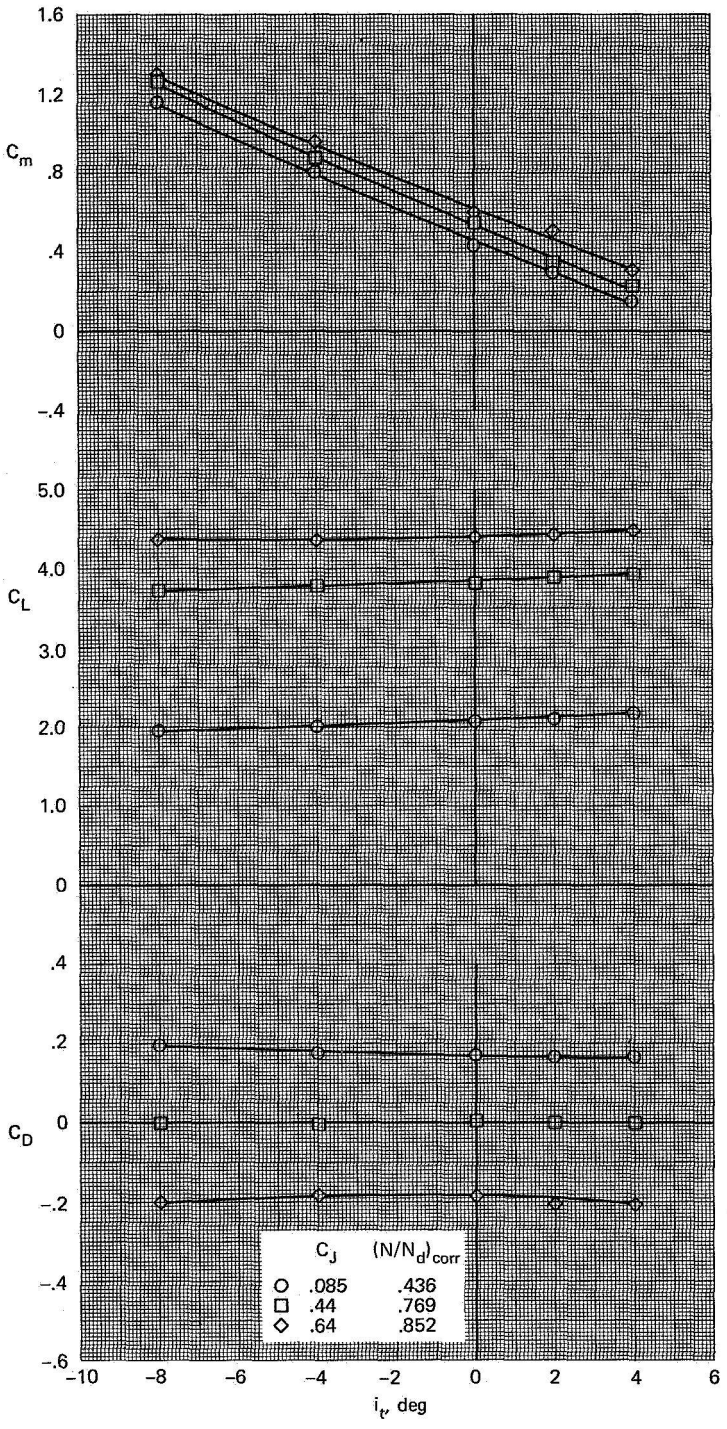

(a) $\delta_f = 40$, $\delta_a = 40/40$, $\alpha = 0$, $q_{nom} = 8.3$

Figure 10.– The effect of horizontal tail deflection on the lift, drag, and pitching moment characteristics of the aircraft.

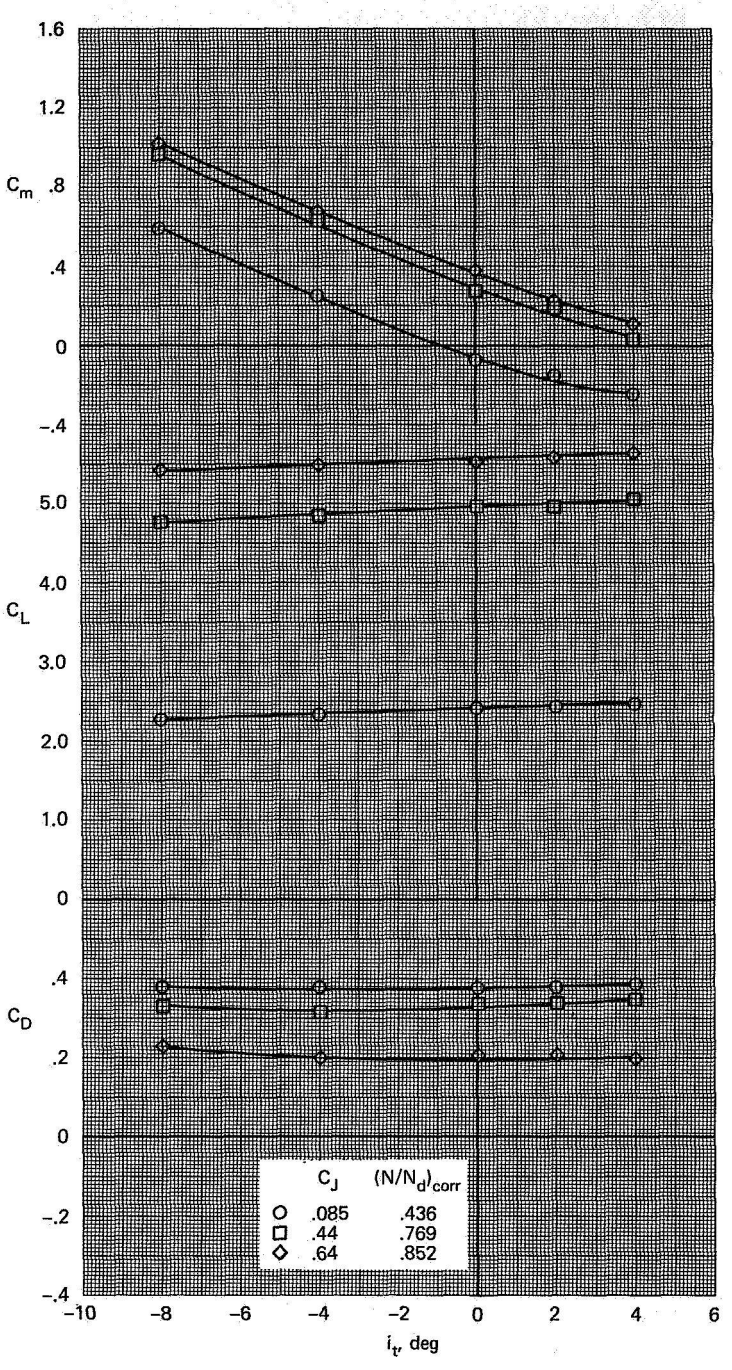

(b) $\delta_f = 40$, $\delta_a = 40/40$, $\alpha = 10$, $q_{nom} = 8.3$

Figure 10.– Continued.

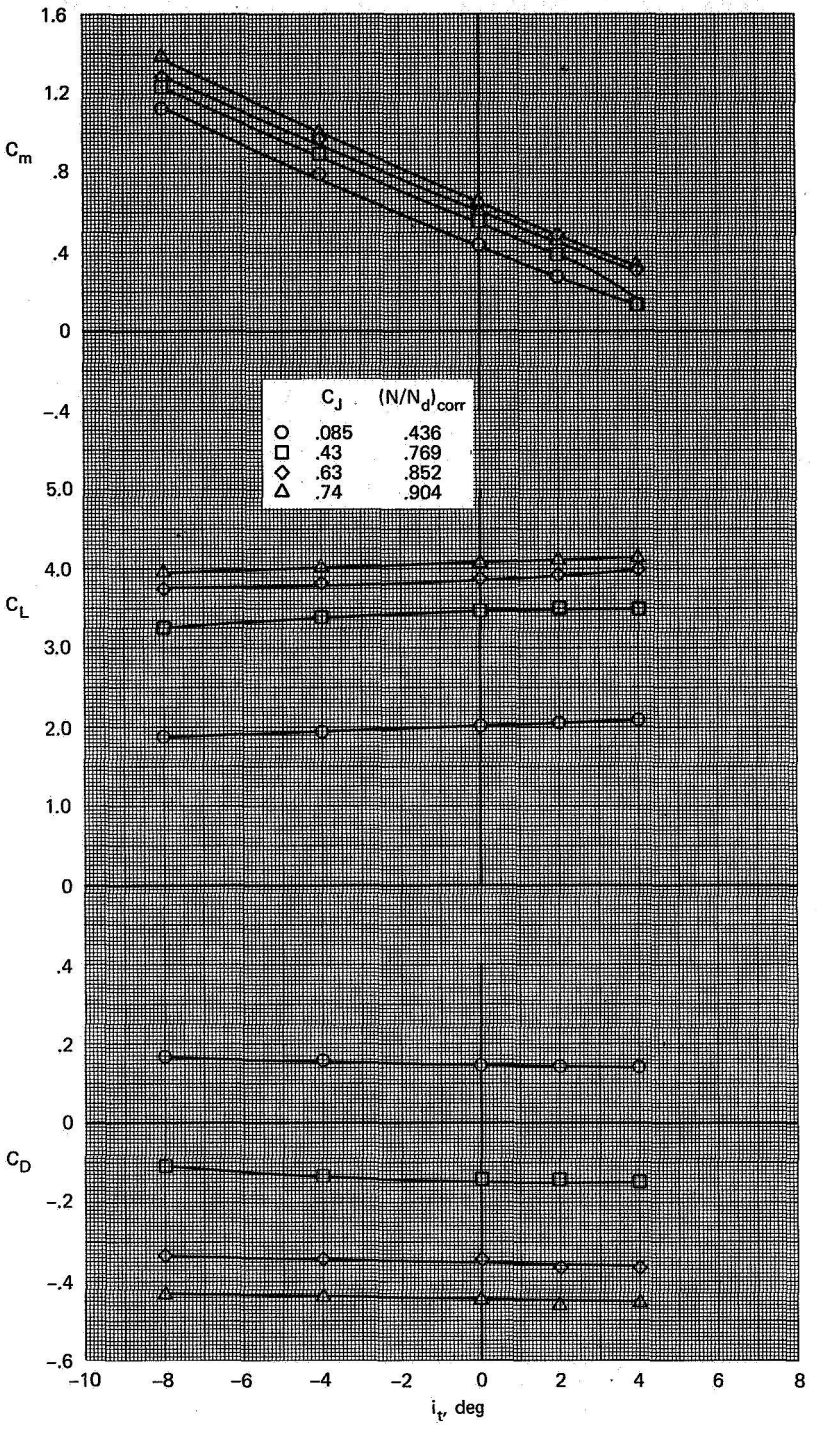

(c) $\delta_f = 30$, $\delta_a = 30/30$, $\alpha = 0$, $q_{nom} = 8.5$

Figure 10.– Continued.

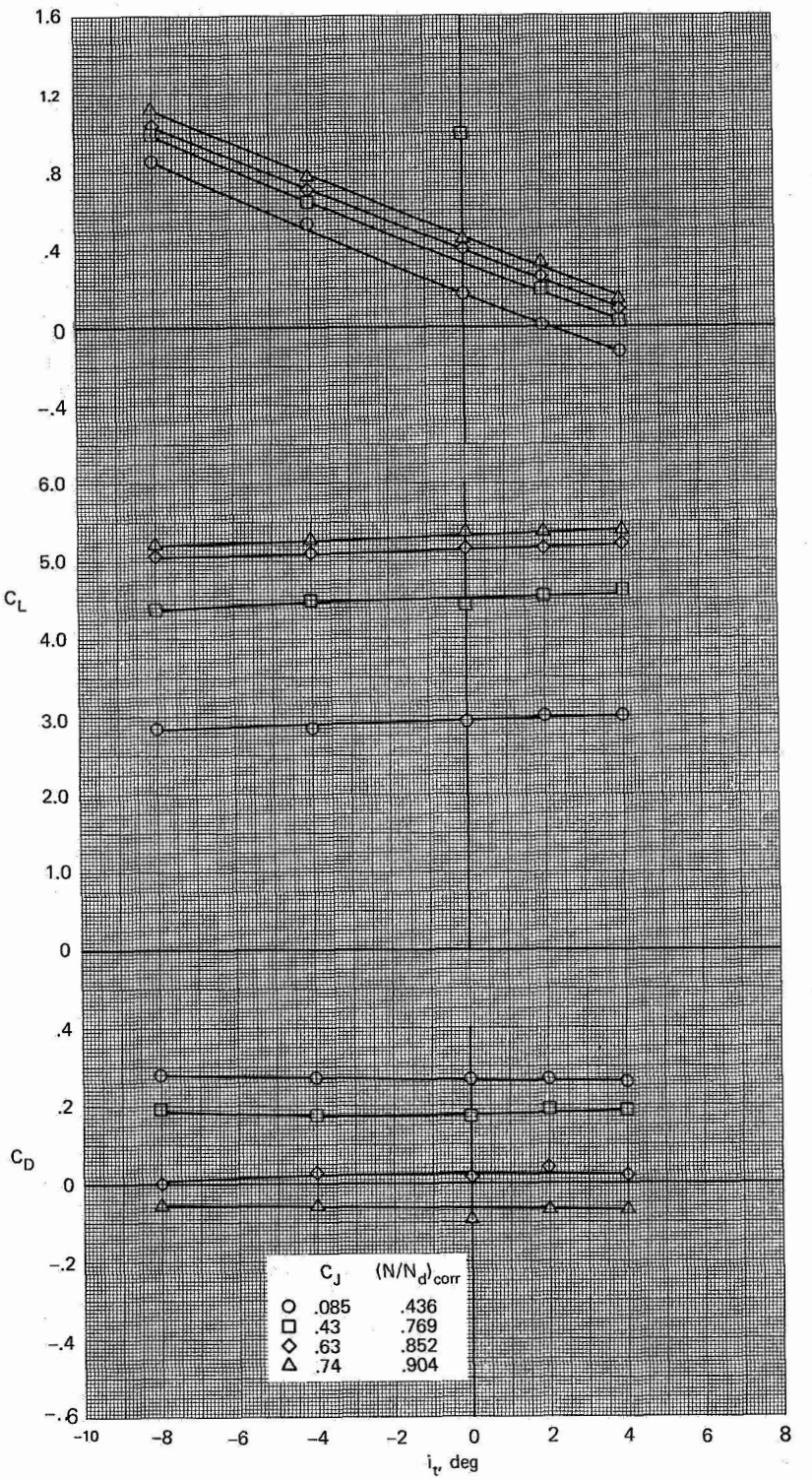

(d) $\delta_f = 30$, $\delta_a = 30/30$, $\alpha = 10$, $q_{nom} = 8.5$

Figure 10.– Continued.

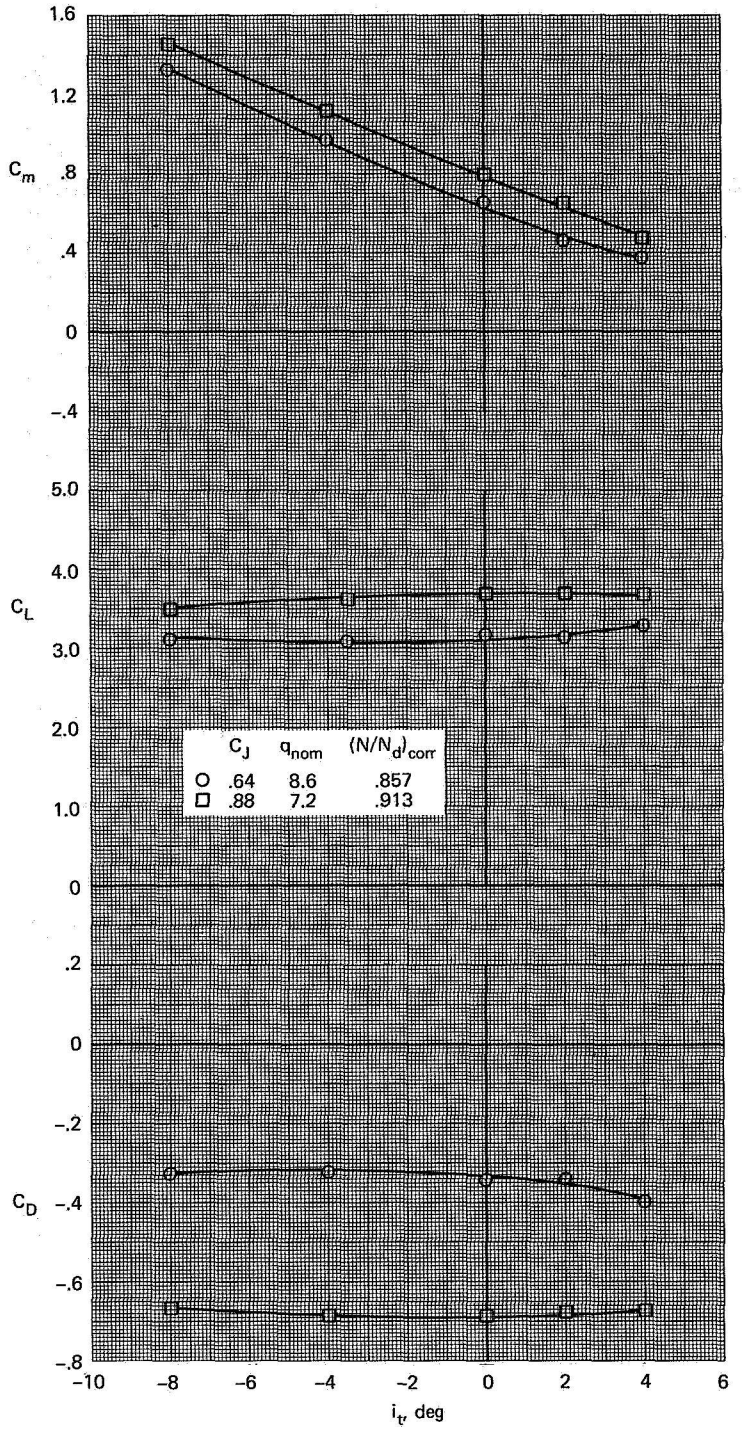

(e) $\delta_f = 40$, $\delta_a = 0/0$, $\alpha = 0$

Figure 10.– Continued.

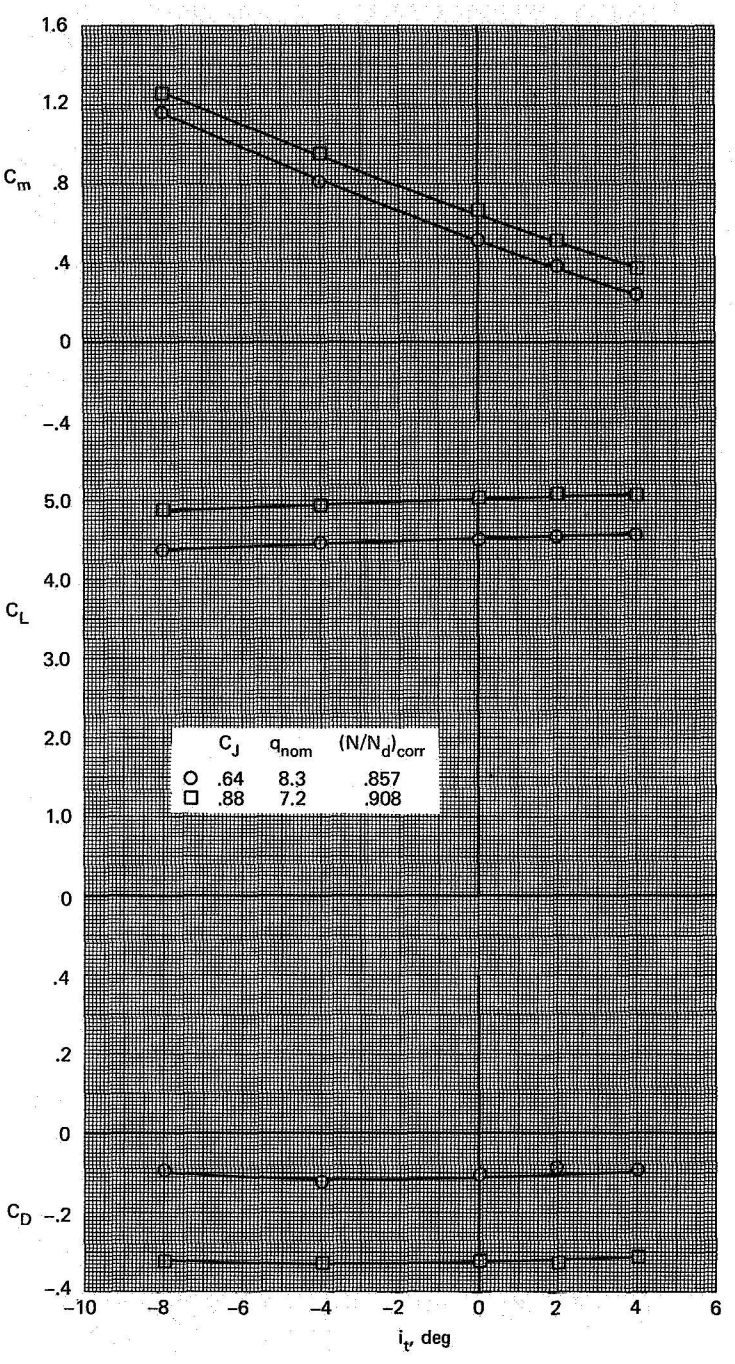

(f) $\delta_f = 40$, $\delta_a = 0/0$, $\alpha = 10$

Figure 10.– Concluded.

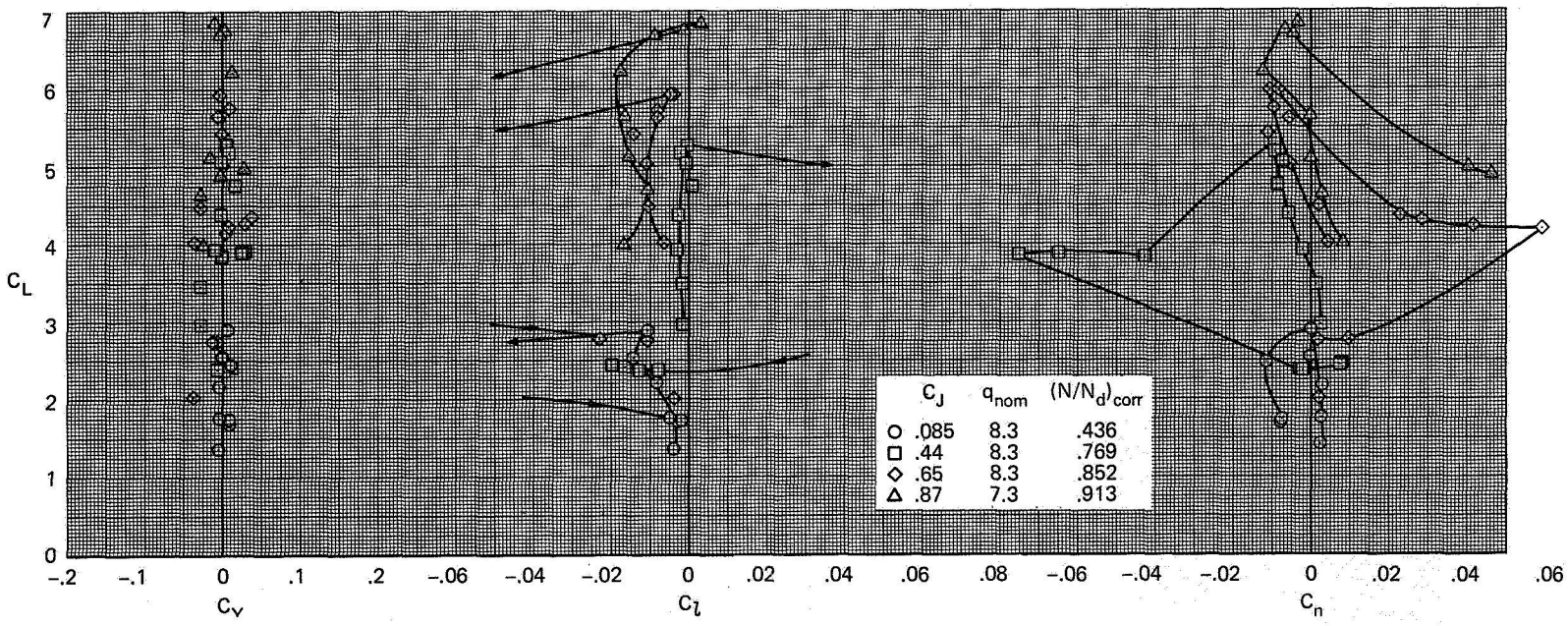

(a) $\delta_f = 40$, $\delta_a = 40/40$

Figure 11.– The effect of C_J on the lateral-directional characteristics of the aircraft; $i_t = 4$.

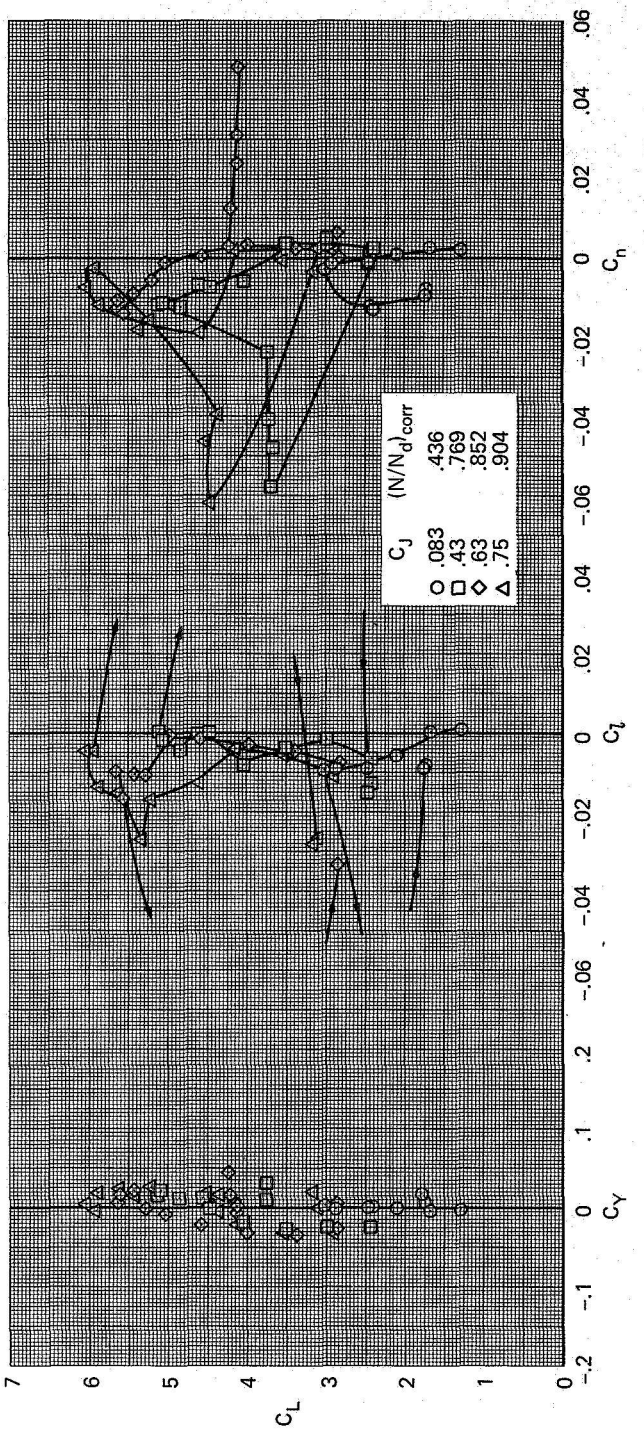

(b) $\delta_f = 30$, $\delta_a = 30/30$, $q_{nom} = 8.5$

Figure 11.– Continued.

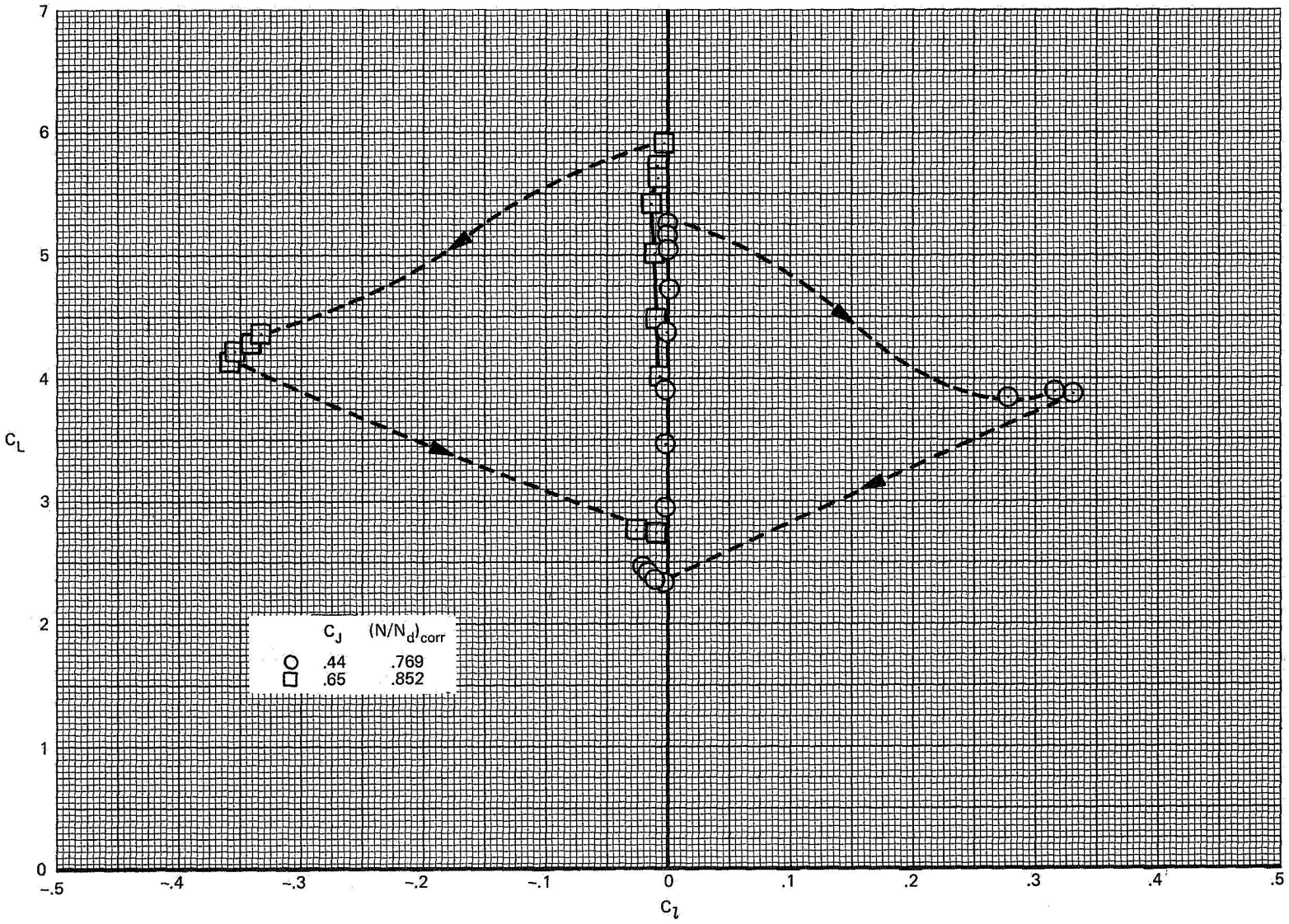

(c) Typical roll characteristics of stall; $\delta_f = 40$, $\delta_a = 40/40$, $\beta = 0$, $q_{nom} = 8.3$.

Figure 11.– Concluded.

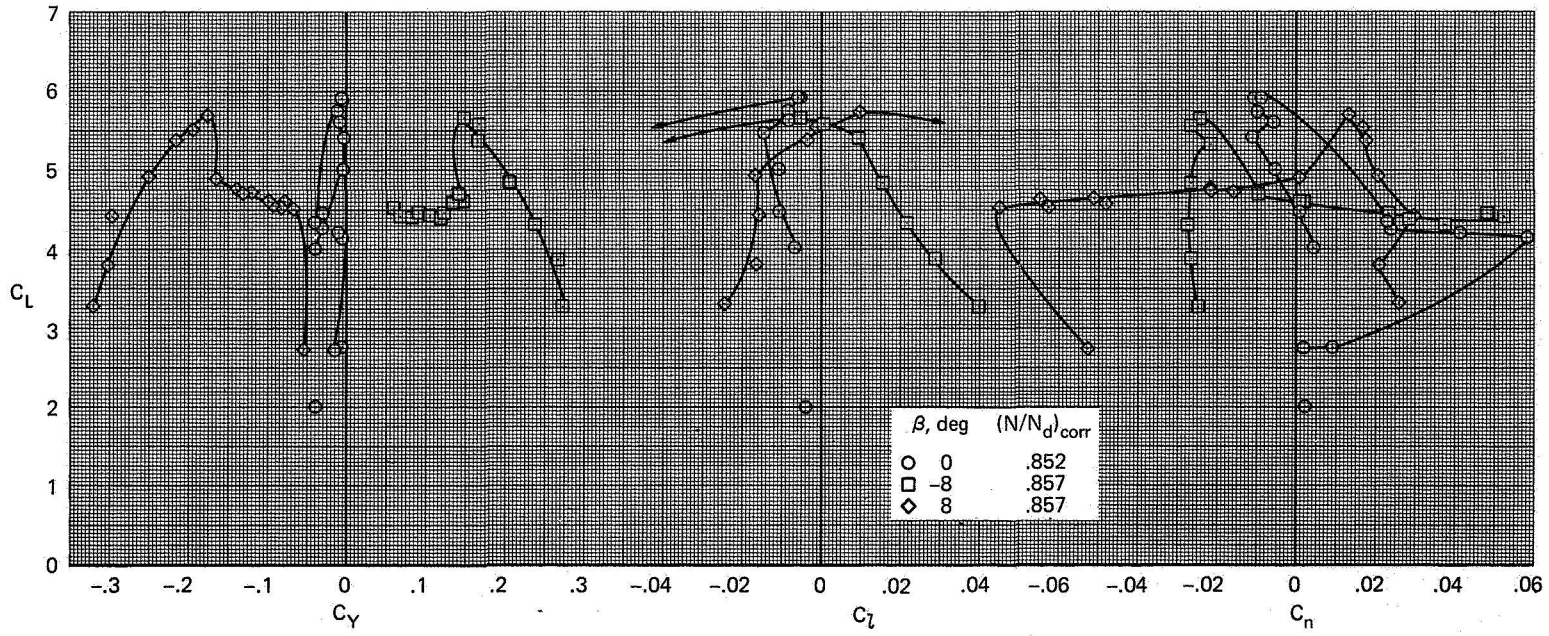

Figure 12.– The effect of sideslip on the lateral-directional characteristics of the aircraft; $\delta_f = 40$, $\delta_a = 40/40$, $i_t = 4$, $C_J = 0.65$, $q_{nom} = 8.3$.

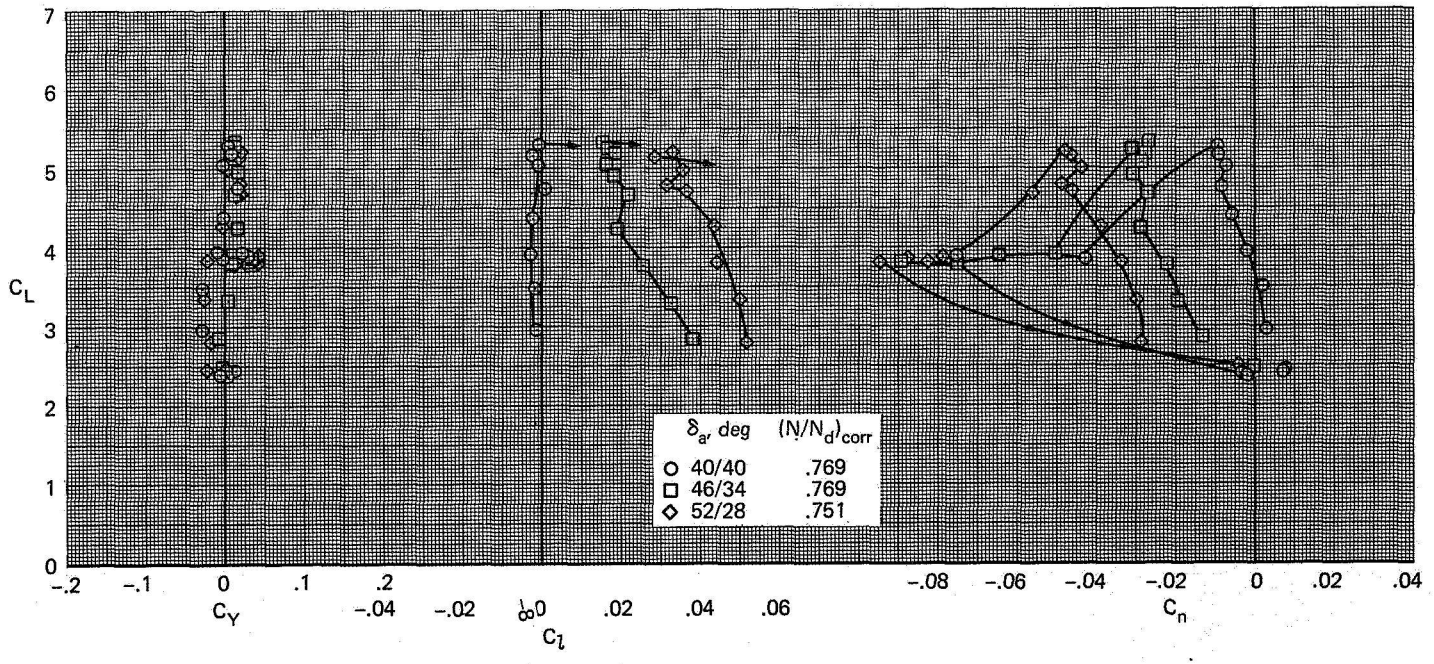

(a) $\delta_f = 40$, $C_J = 0.44$, $q_{nom} = 8.4$

Figure 13.– The effect of asymmetric aileron deflection on the lateral-directional characteristics of the aircraft; $i_t = 4$.

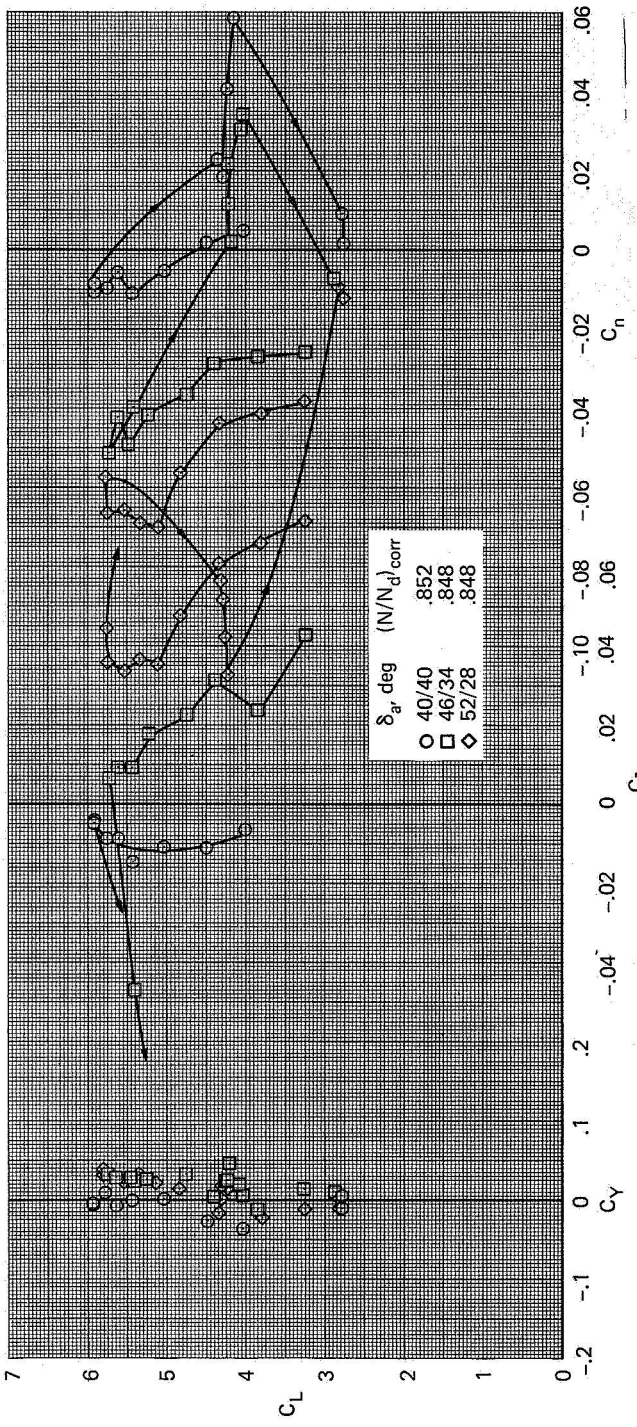

(b) $\delta_f = 40$, $C_J = 0.63$, $q_{nom} = 8.5$

Figure 13.– Continued.

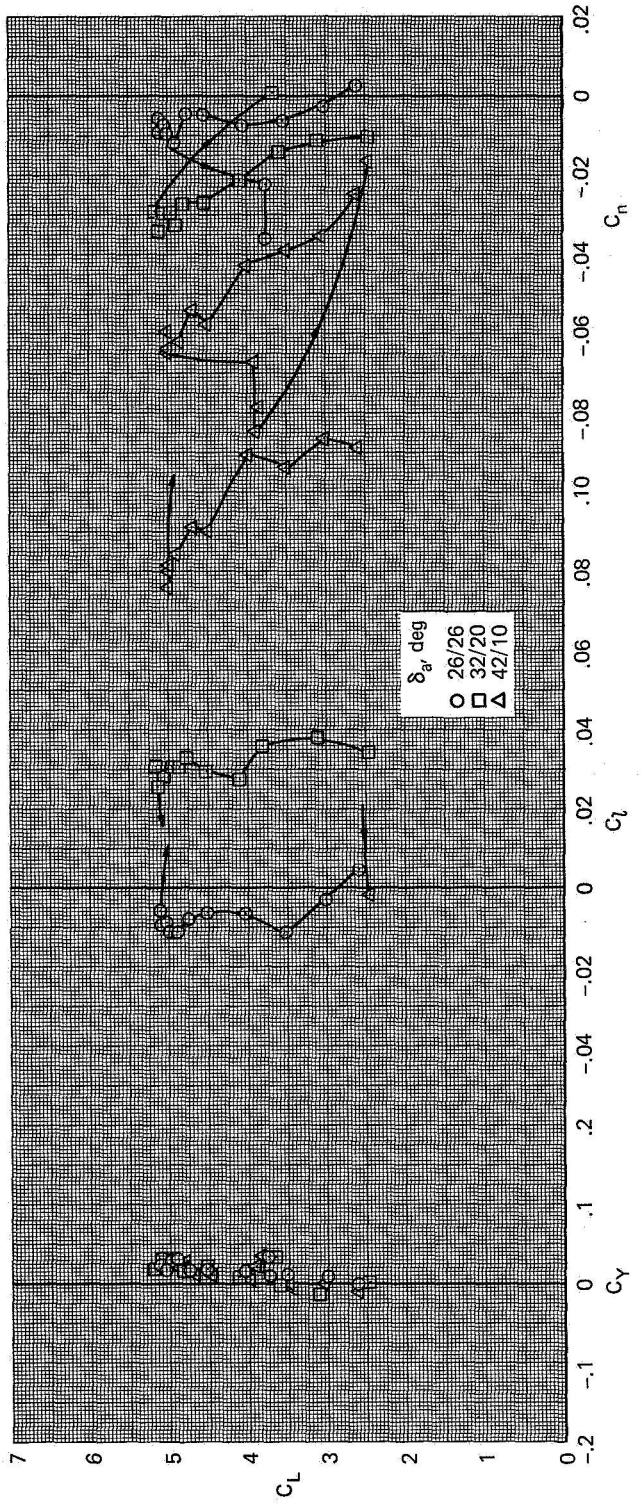

(c) $\delta_f = 40$, $C_J = 0.43$, $q_{nom} = 8.5$, $(N/Nd)_{corr} = 0.782$

Figure 13.– Continued.

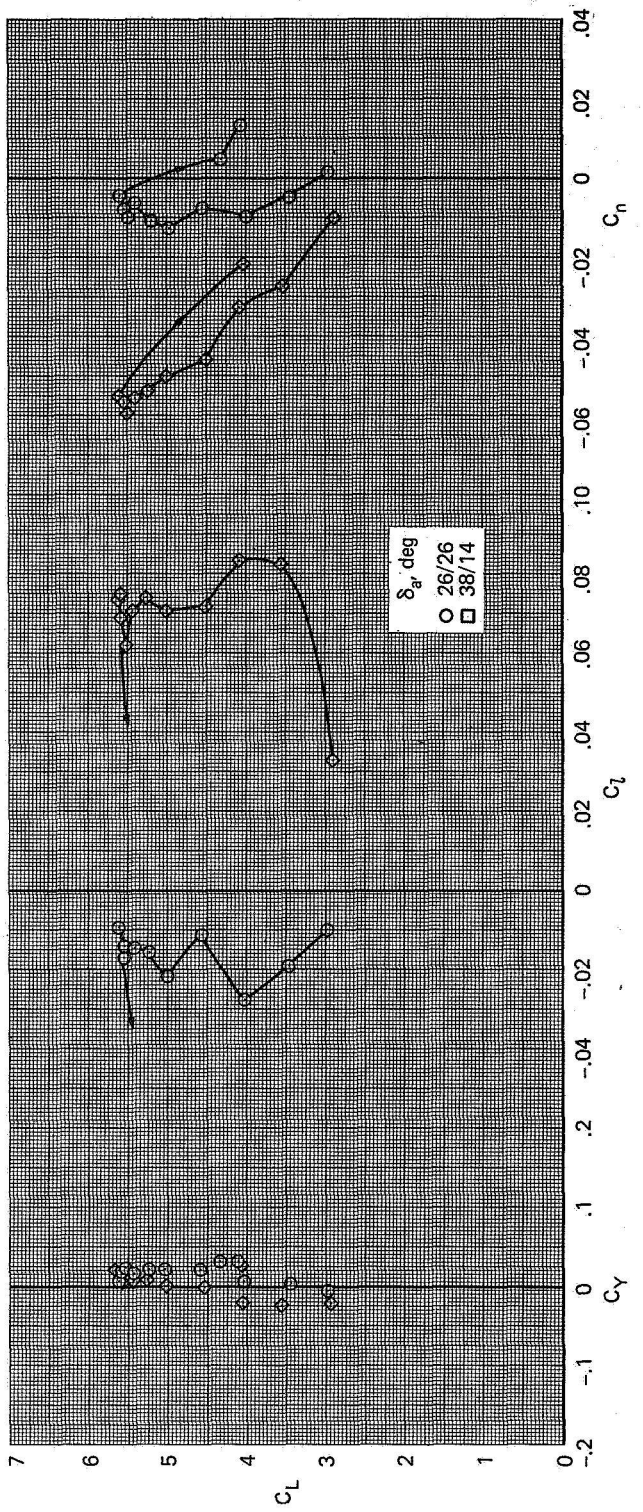

(d) $\delta_f = 40$, $C_J = 0.63$, $q_{nom} = 8.5$, $(N/Nd)_{corr} = 0.865$

Figure 13.– Continued.

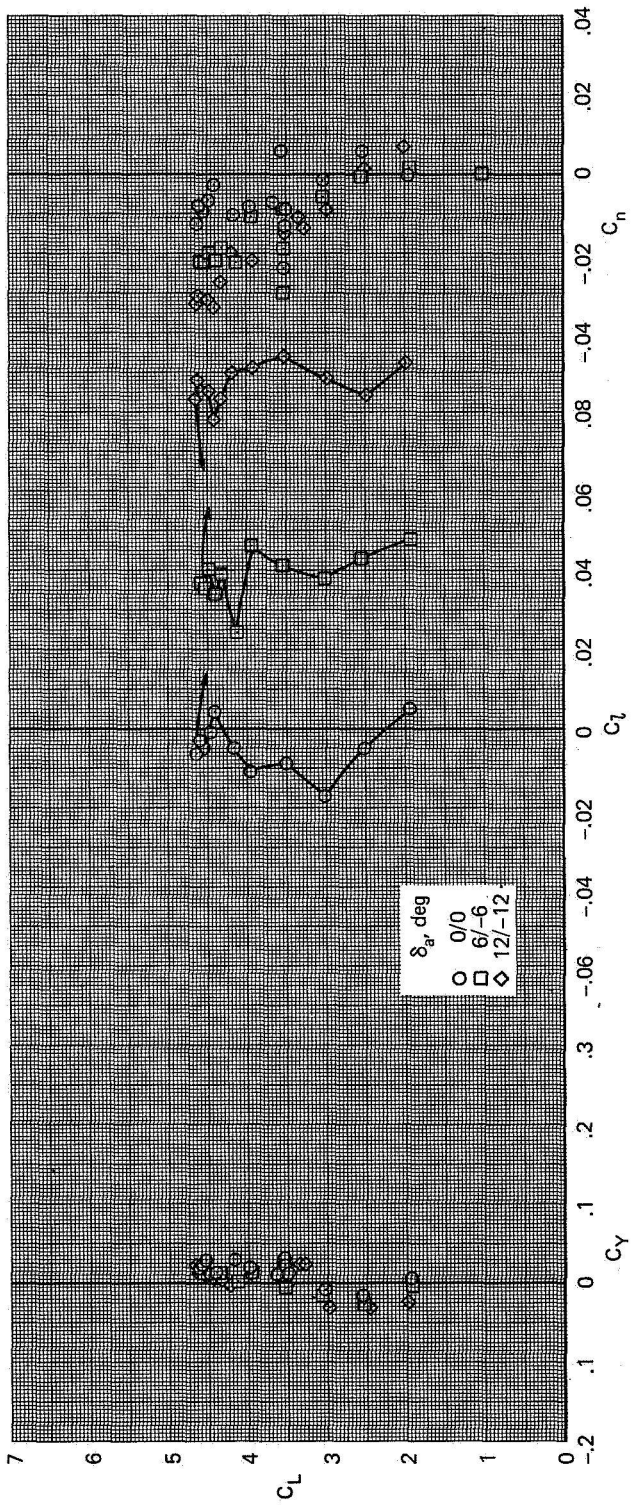

(e) $\delta_f = 40$, $C_J = 0.43$, $q_{nom} = 8.5$, $(N/Na)_{corr} = 0.782$

Figure 13.– Continued.

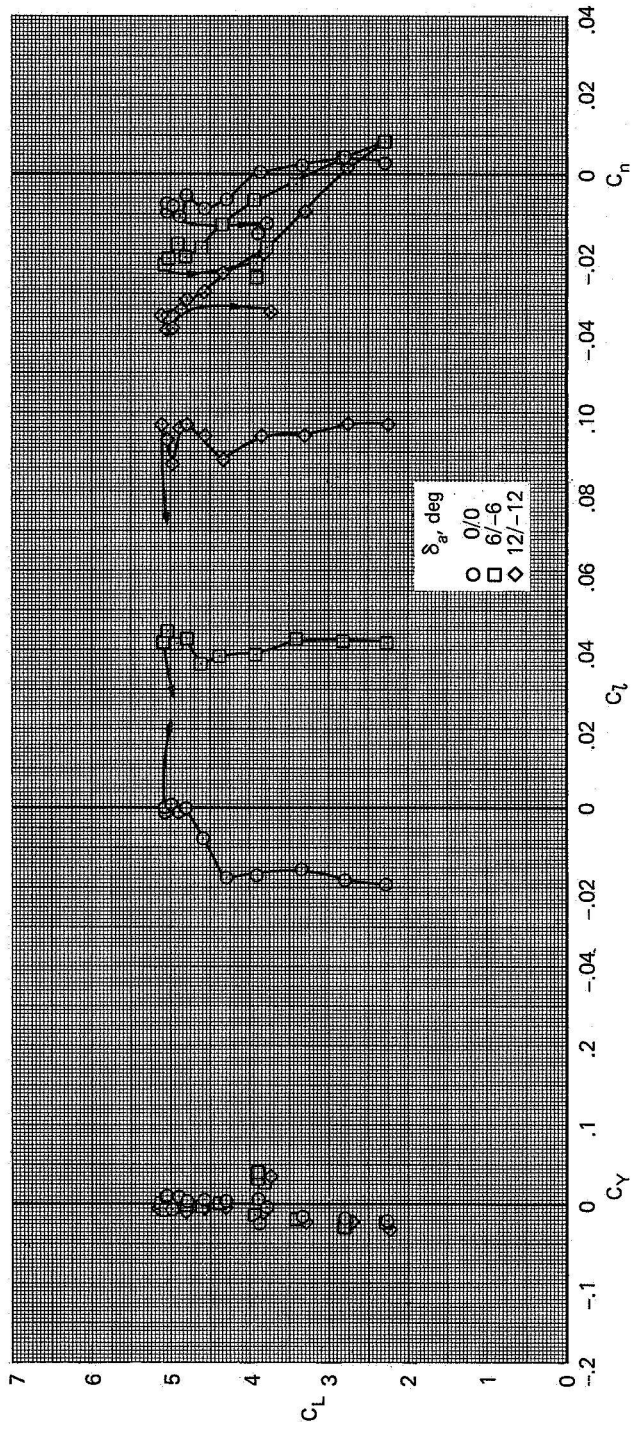

(f) $\delta_f = 40$, $C_J = 0.63$, $q_{nom} = 8.5$, $(N/Nd)_{corr} = 0.865$

Figure 13.– Continued.

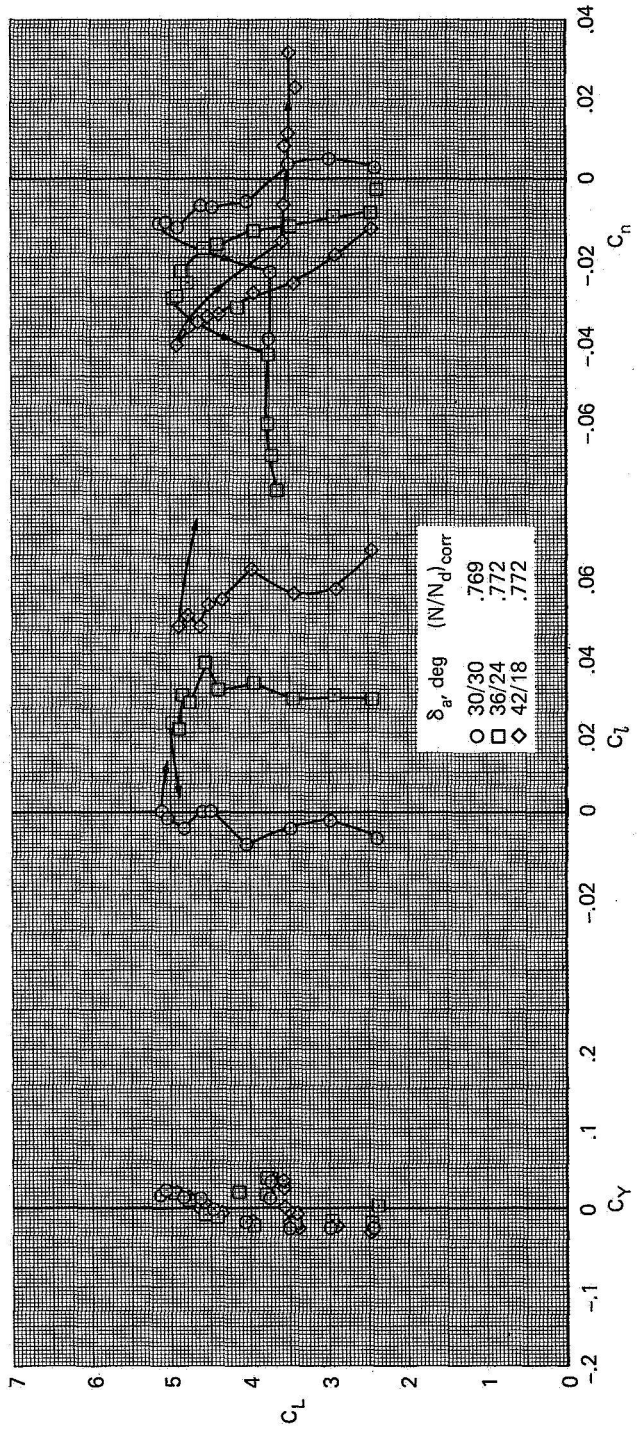

(g) $\delta_f = 30$, $C_J = 0.43$, $q_{nom} = 8.5$

Figure 13.– Continued.

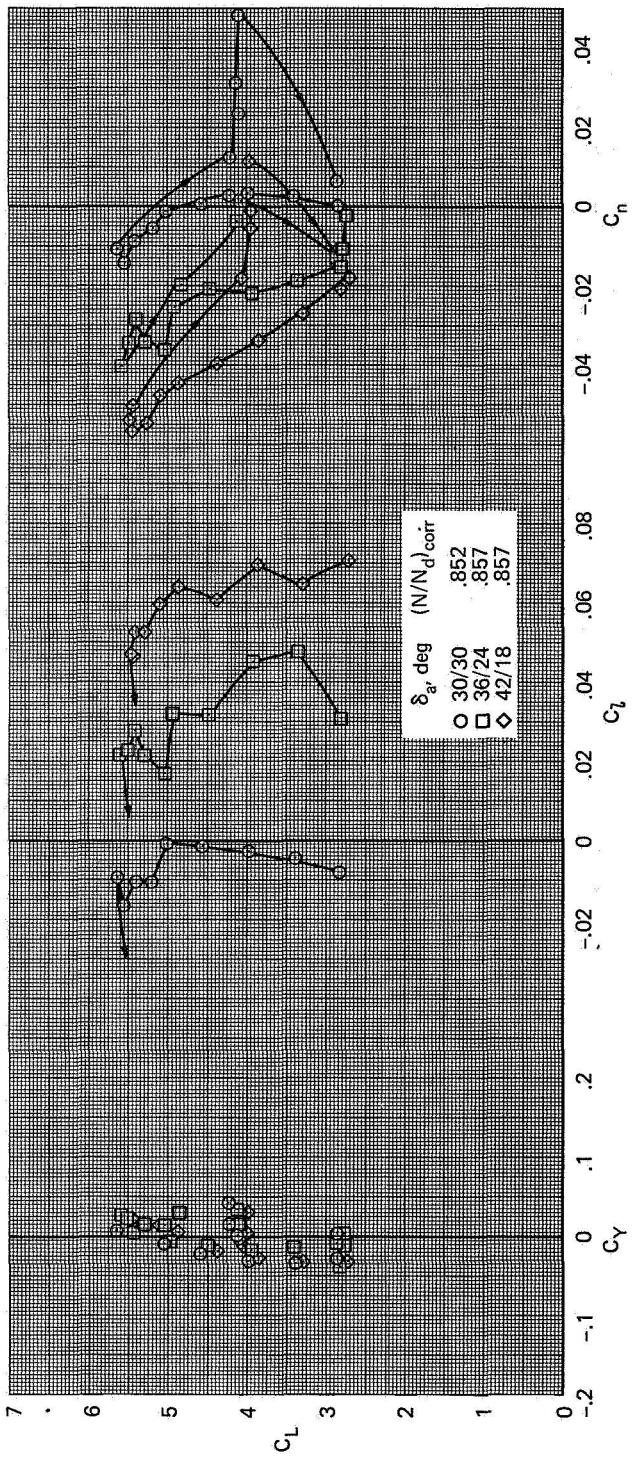

(h) $\delta_f = 30$, $C_J = 0.63$, $q_{nom} = 8.5$

Figure 13.– Concluded.

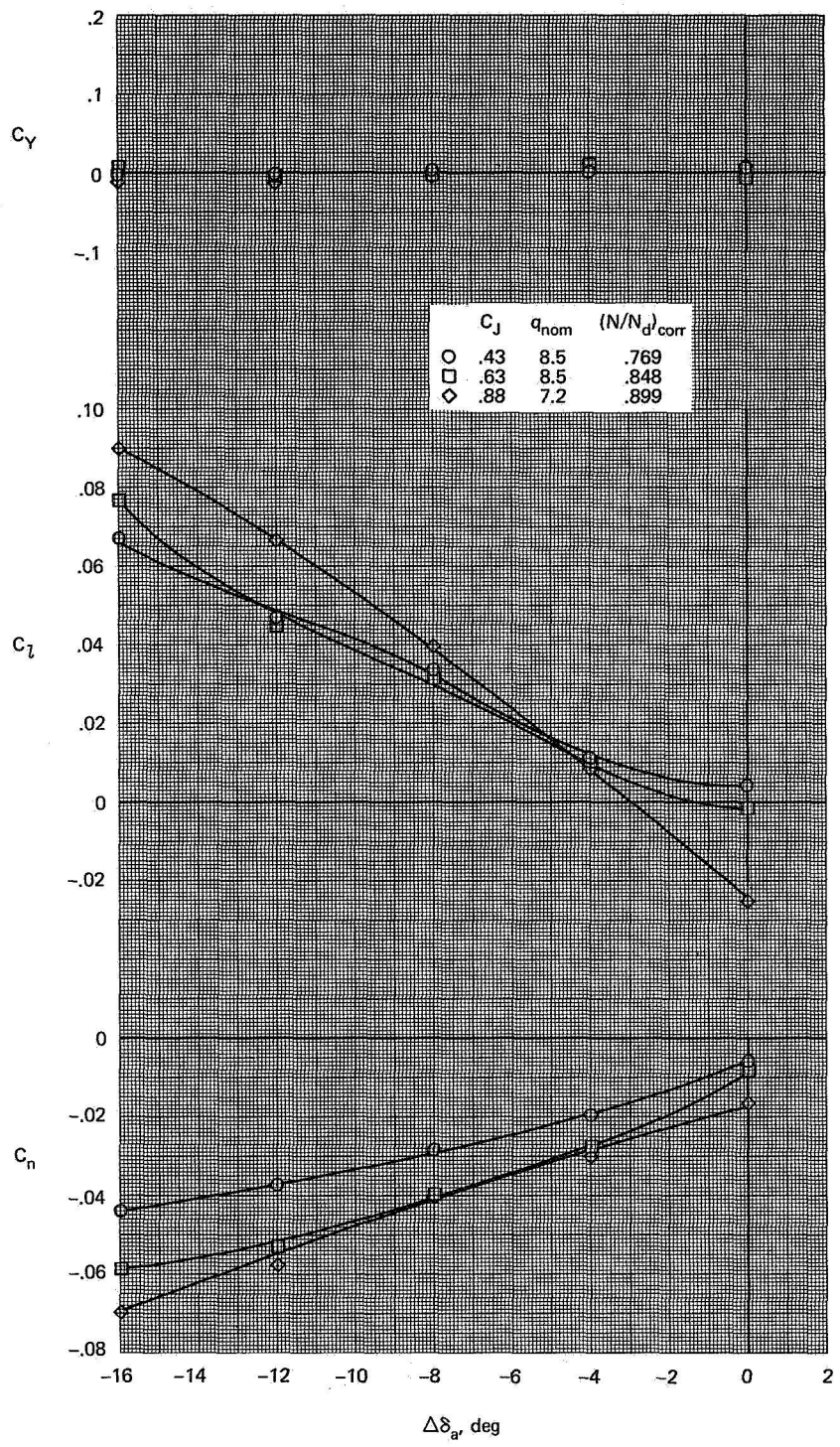

(a) $\delta_f = 40$, $\delta_{a_{nom}} = 40/40$, $\alpha = 0$

Figure 14.– The effect of C_J on the lateral-directional coefficients with varying asymmetric aileron deflection; $i_t = 4$.

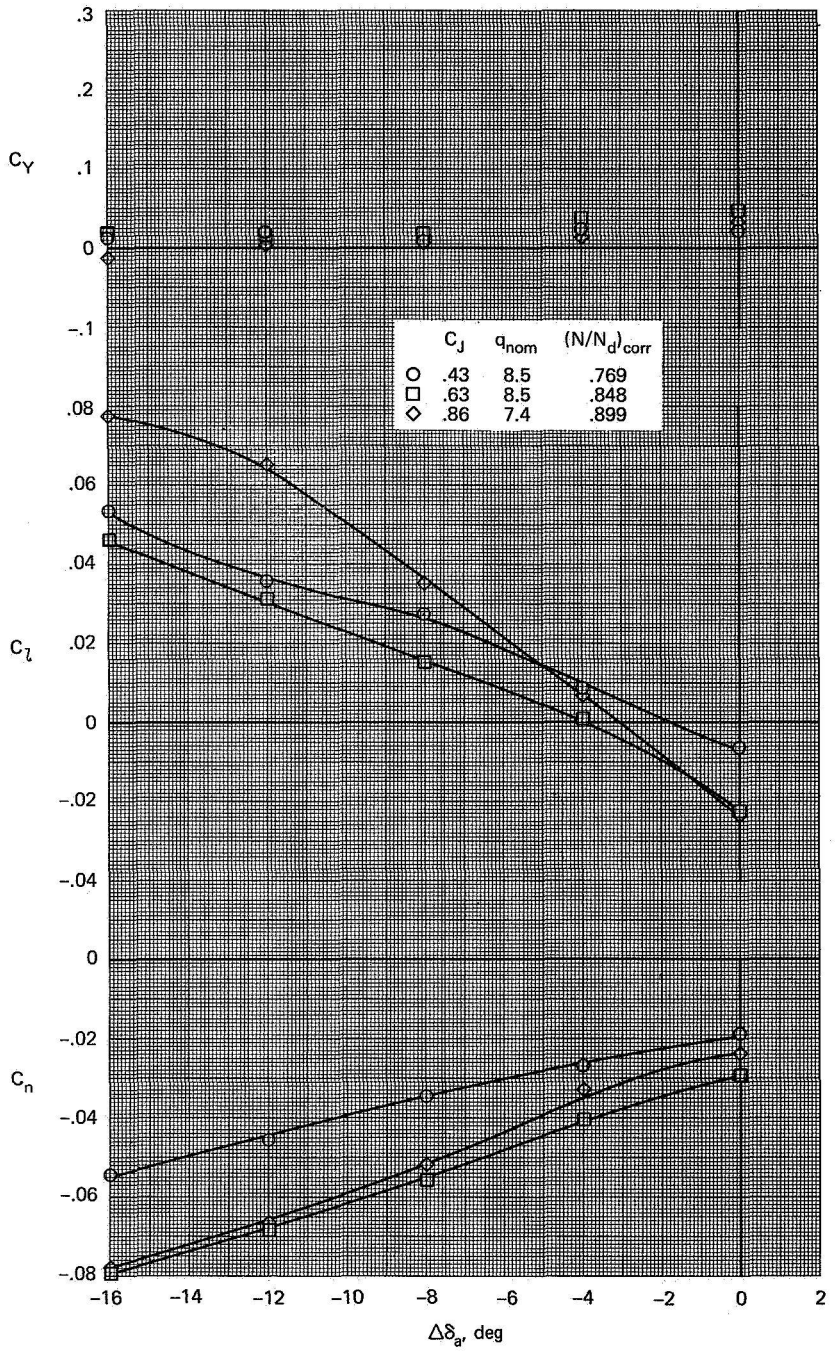

(b) $\delta_f = 40$, $\delta_{a_{nom}} = 40/40$, $\alpha = 10$

Figure 14.– Continued.

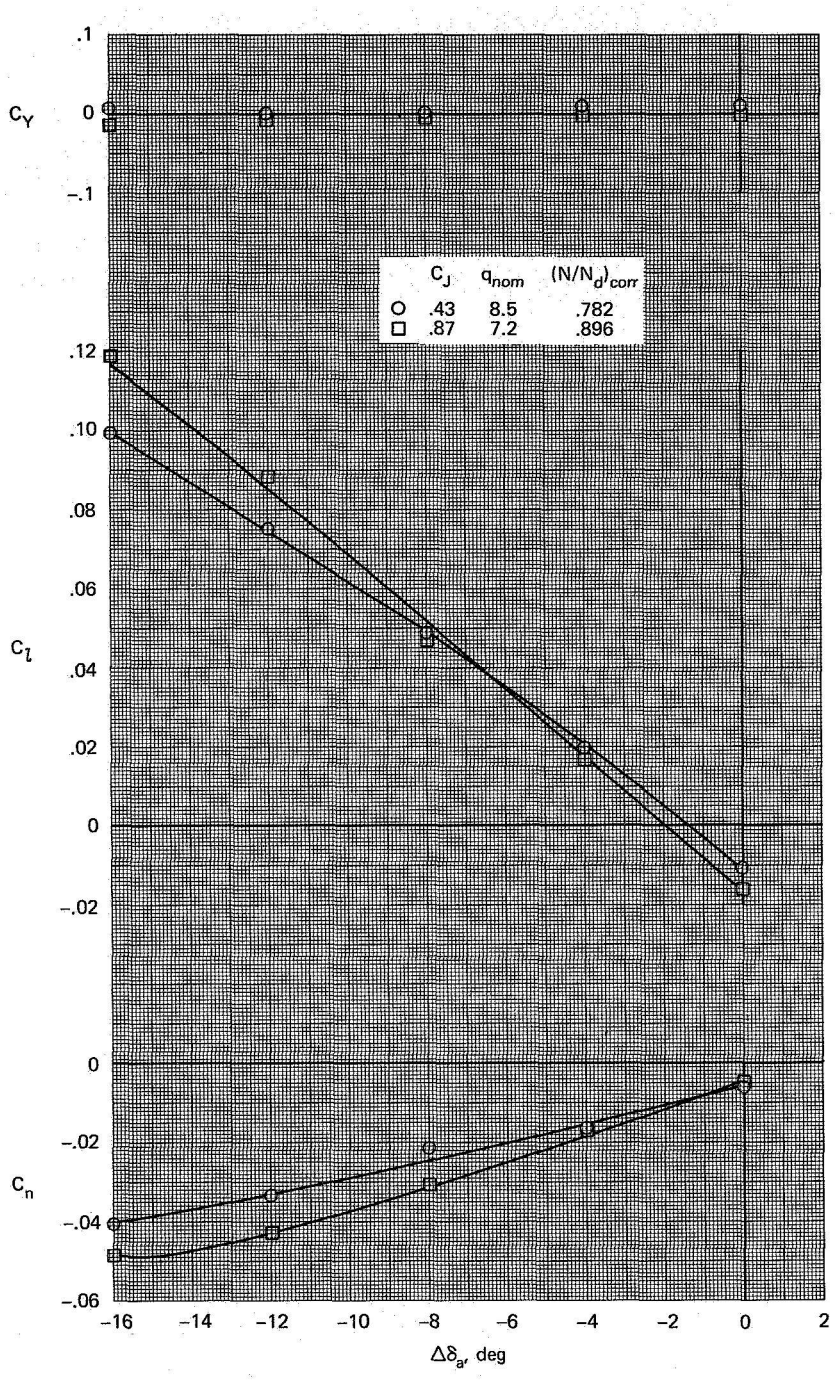

(c) $\delta_f = 40$, $\delta_{a_{nom}} = 26/26$, $\alpha = 0$

Figure 14.– Continued.

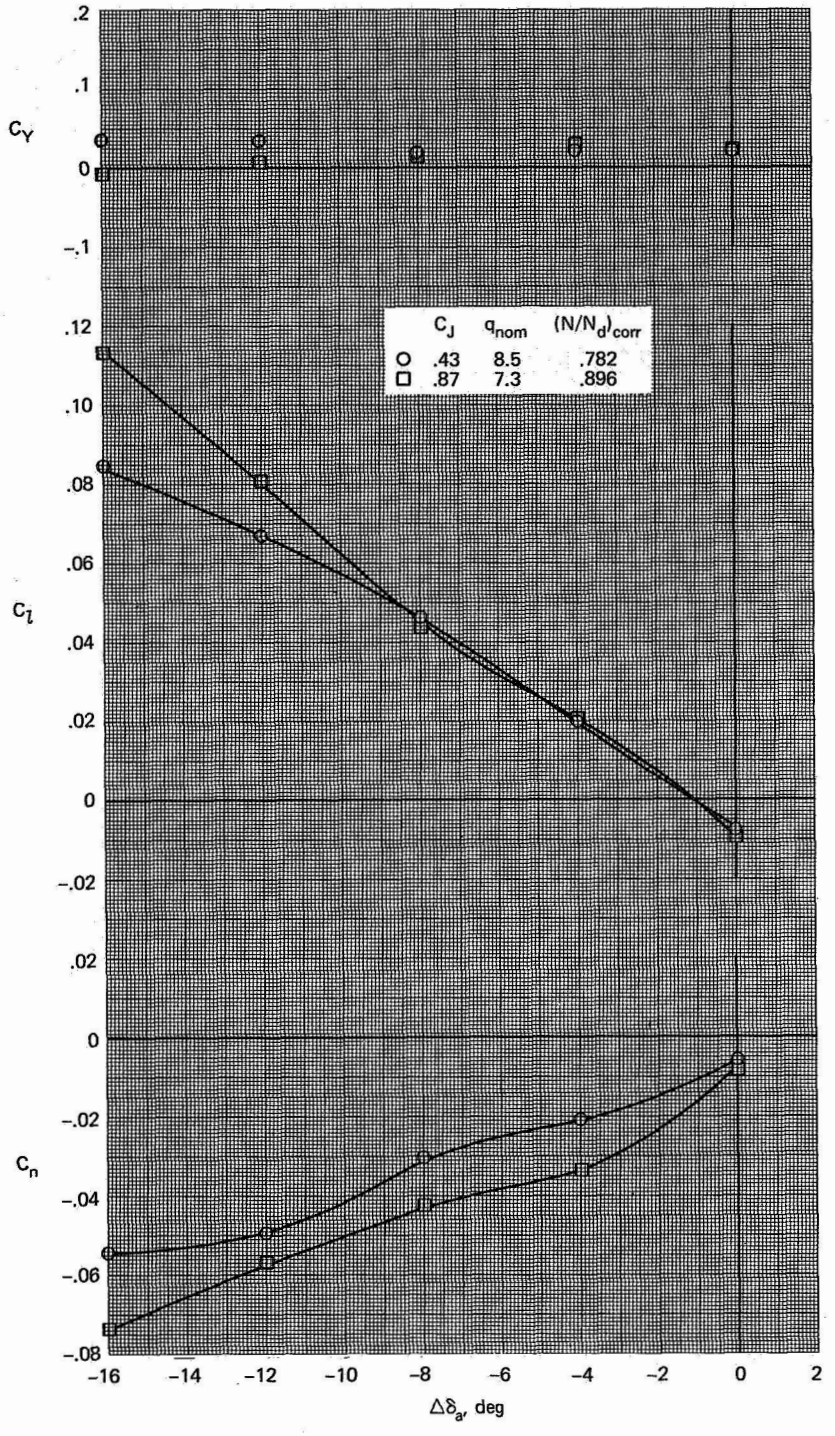

(d) $\delta_f = 40$, $\delta_{a_{nom}} = 26/26$, $\alpha = 10$

Figure 14.– Continued.

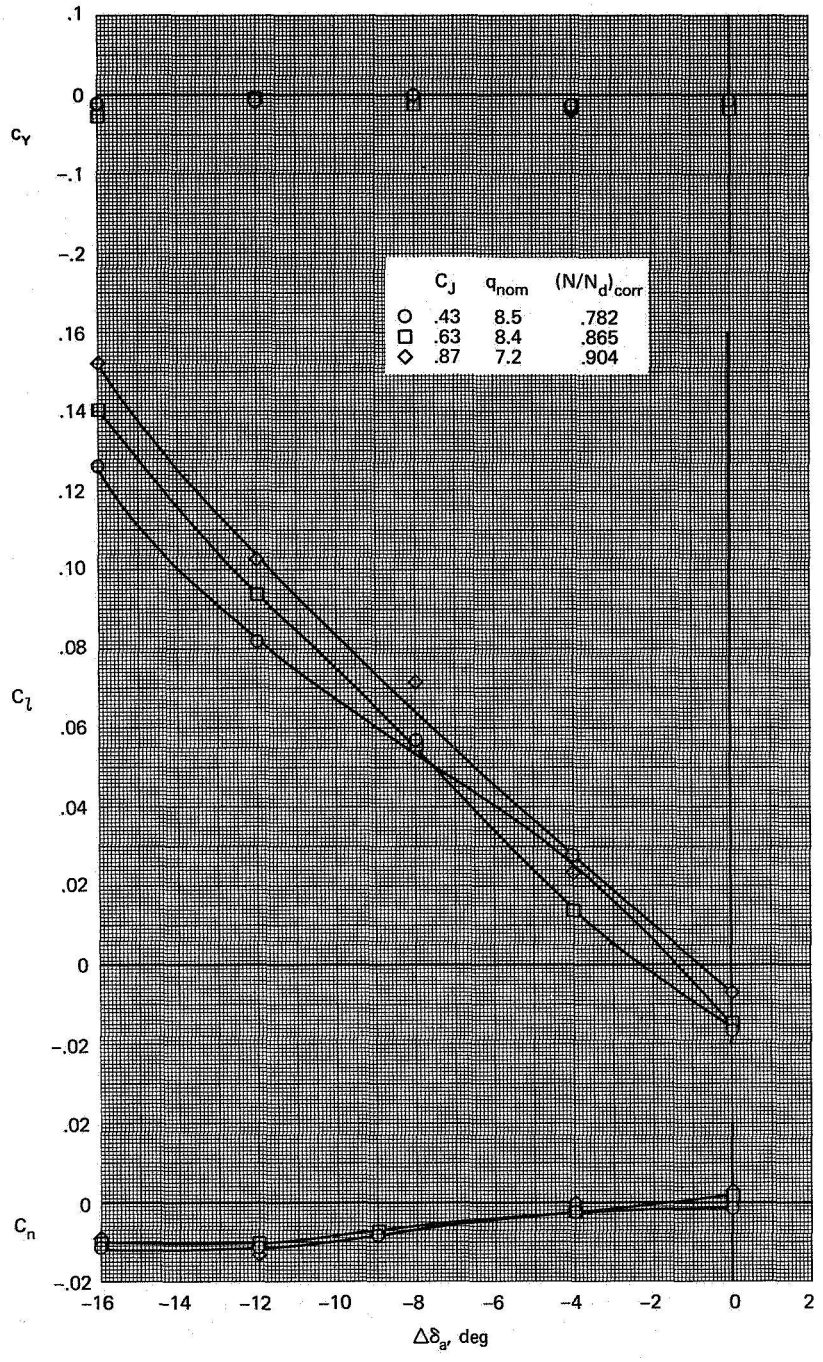

(e) $\delta_f = 40$, $\delta_{a_{nom}} = 0/0$, $\alpha = 0$

Figure 14.– Continued.

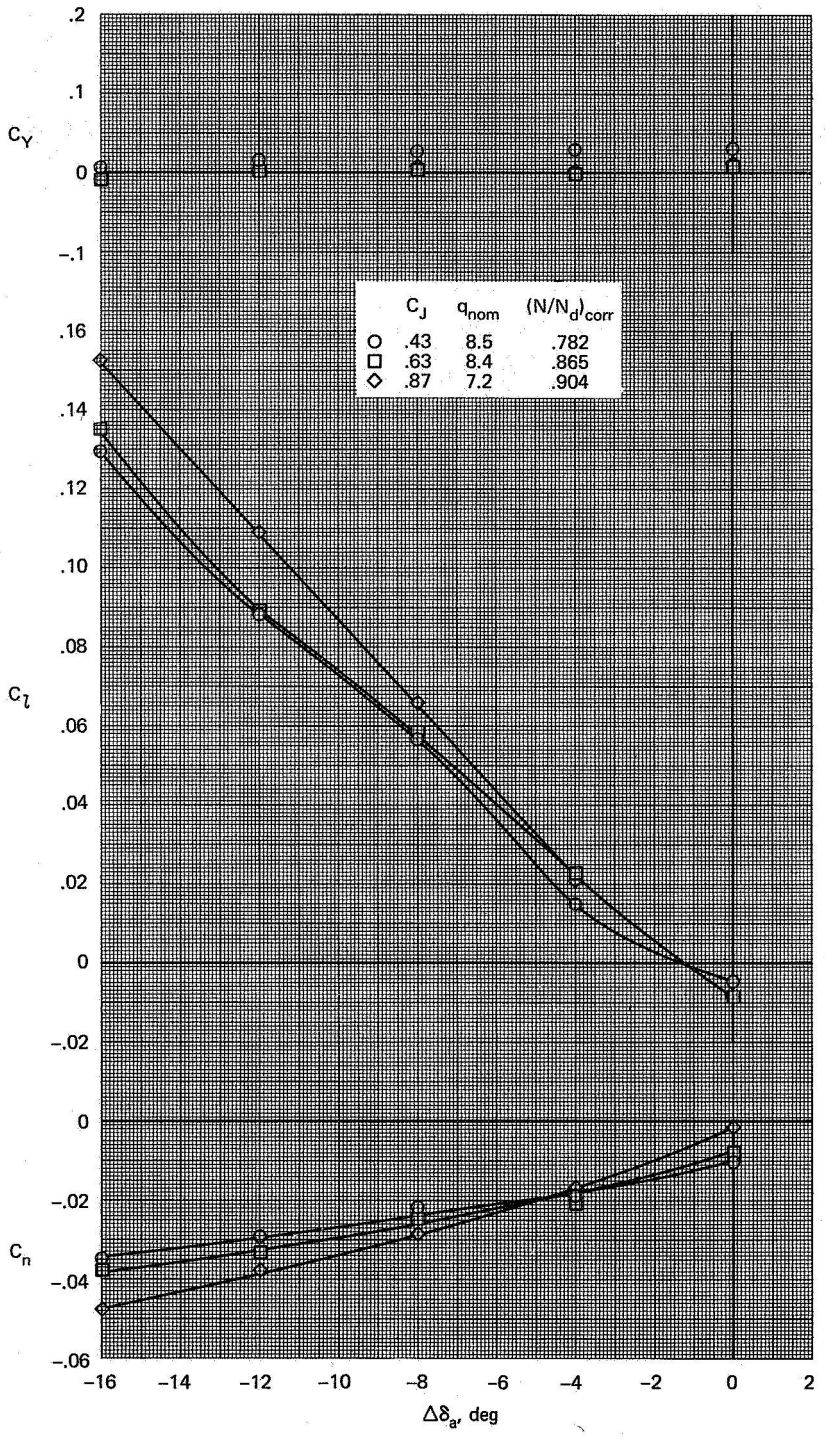

(f) $\delta_f = 40$, $\delta_{a_{nom}} = 0/0$, $\alpha = 10$

Figure 14.– Continued.

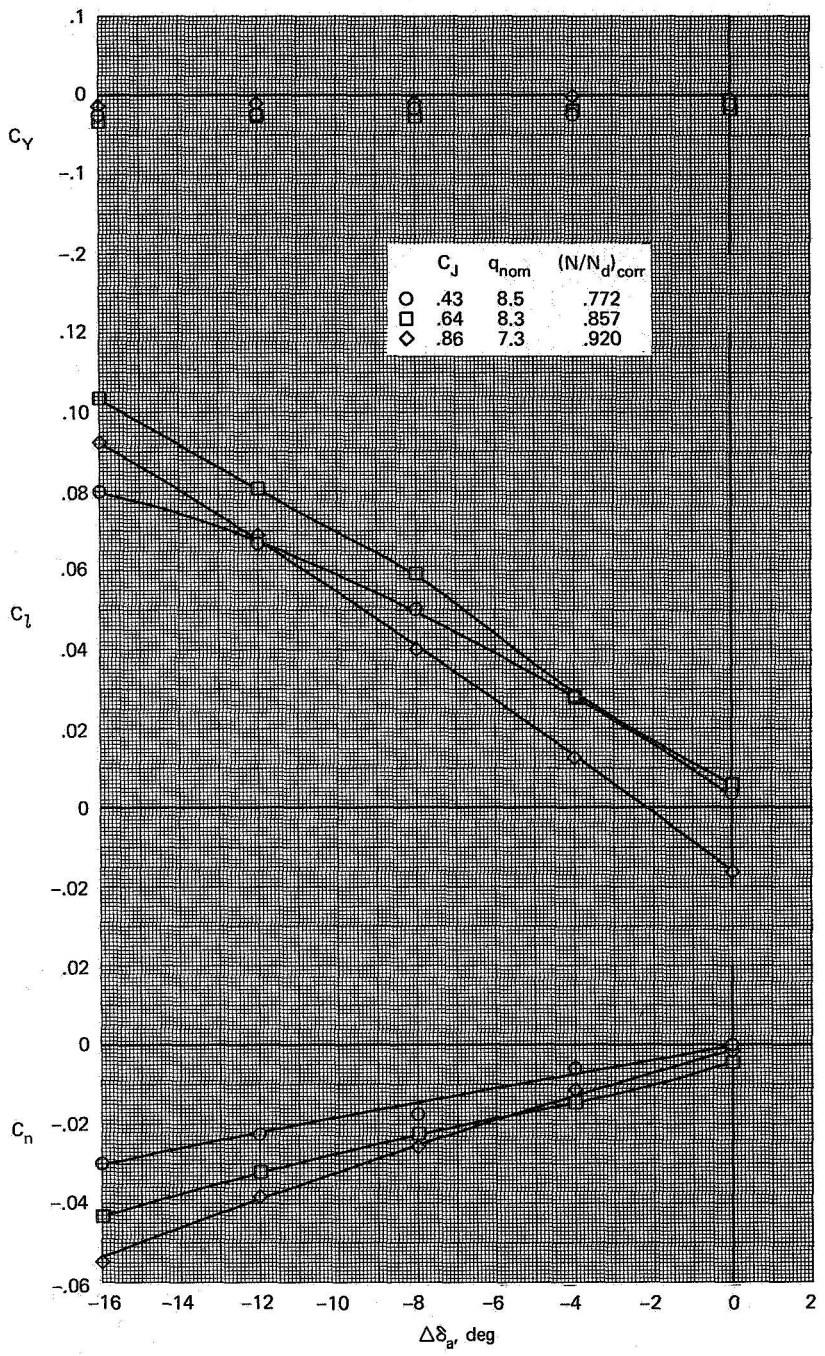

(g) $\delta_f = 30$, $\delta_{a_{nom}} = 30/30$, $\alpha = 0$

Figure 14.– Continued.

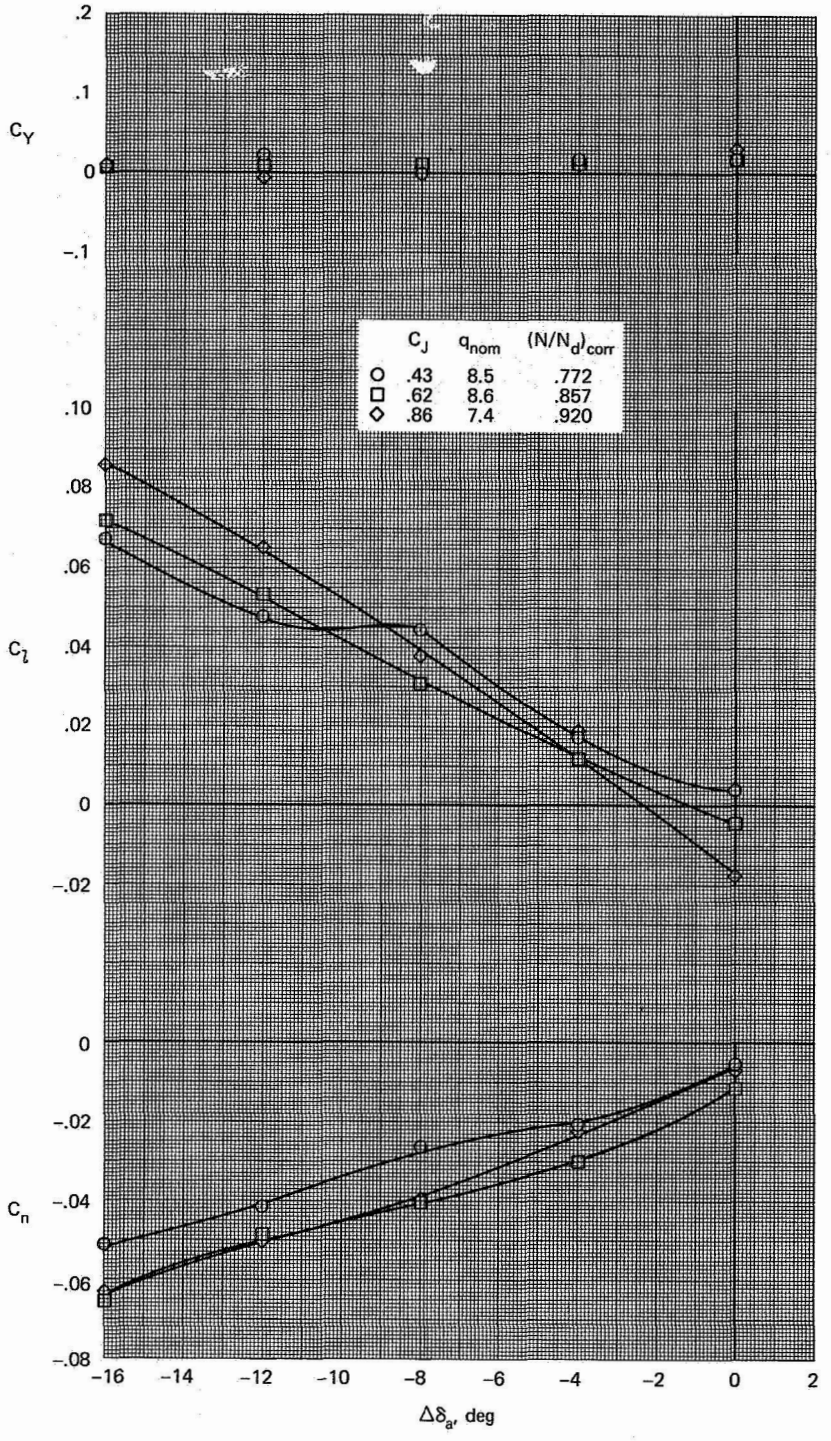

(h) $\delta_f = 30$, $\delta_{a_{nom}} = 30/30$, $\alpha = 10$

Figure 14.– Concluded.

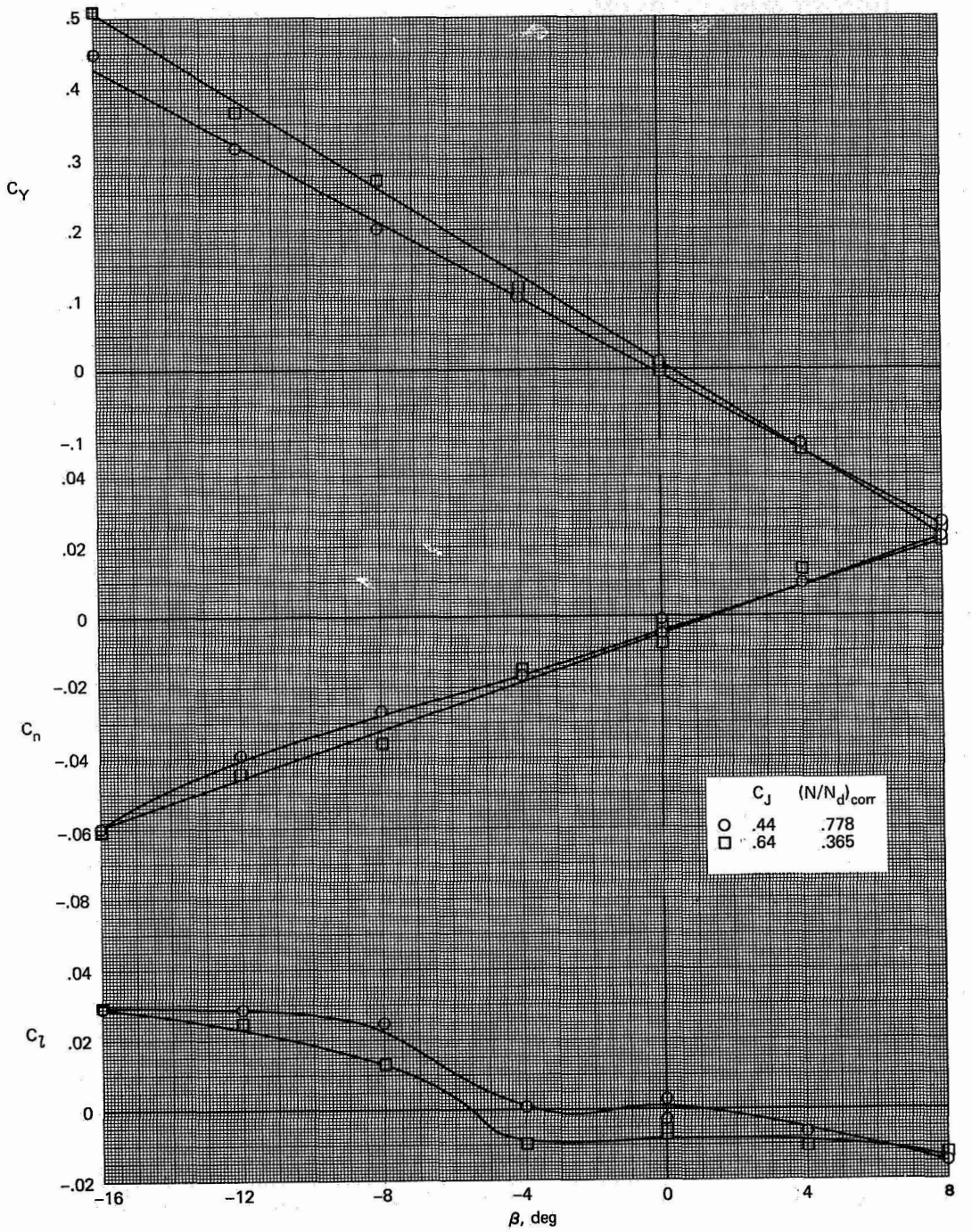

(a) $\delta_f = 40$, $\delta_a = 40/40$, $\alpha = 0$, $q_{nom} = 8.3$

Figure 15.– The effect of C_J on the lateral-directional characteristics with varying sideslip; $i_t = 4$.

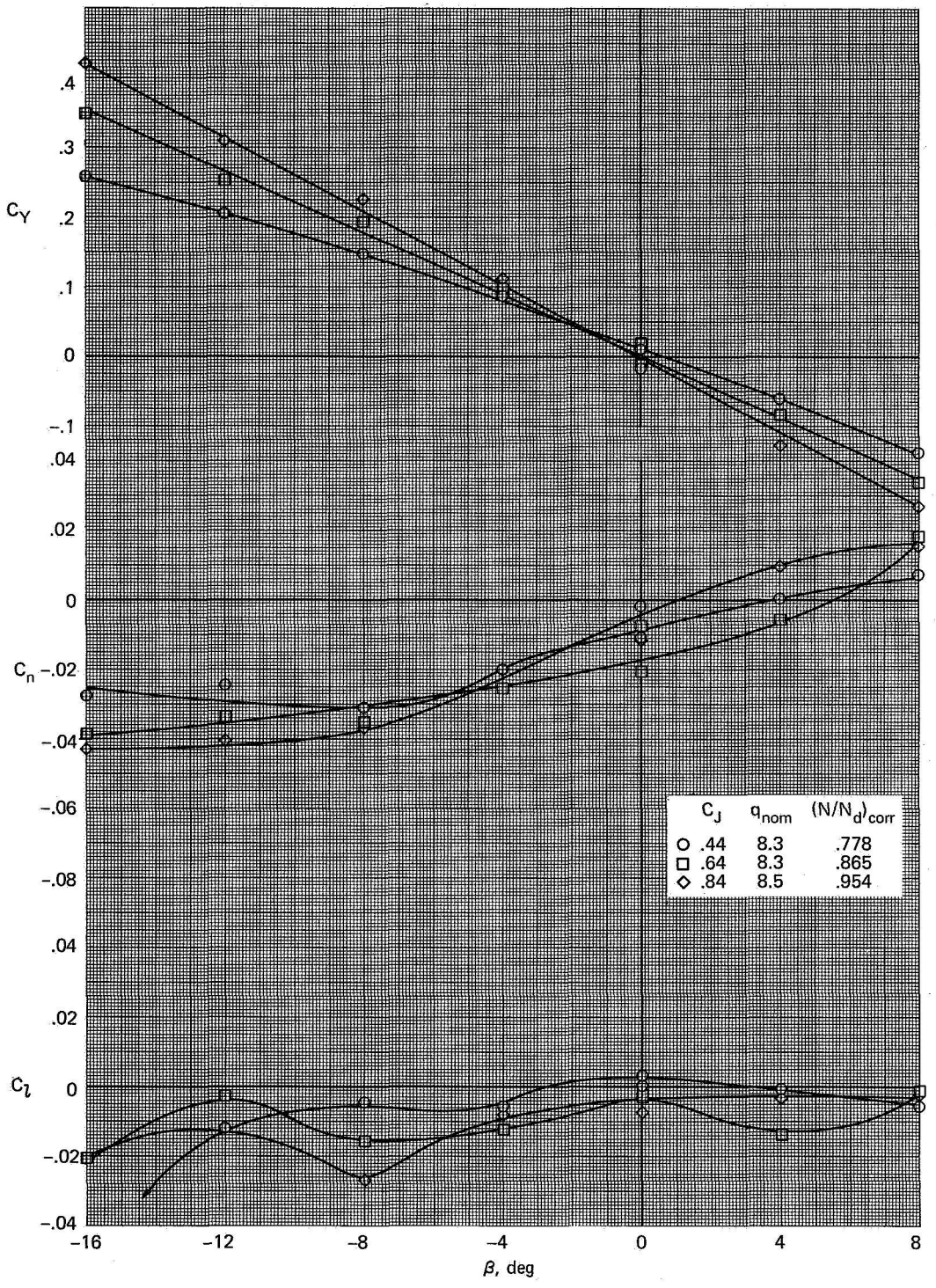

(b) $\delta_f = 40$, $\delta_a = 40/40$, $\alpha = 10$

Figure 15.– Continued.

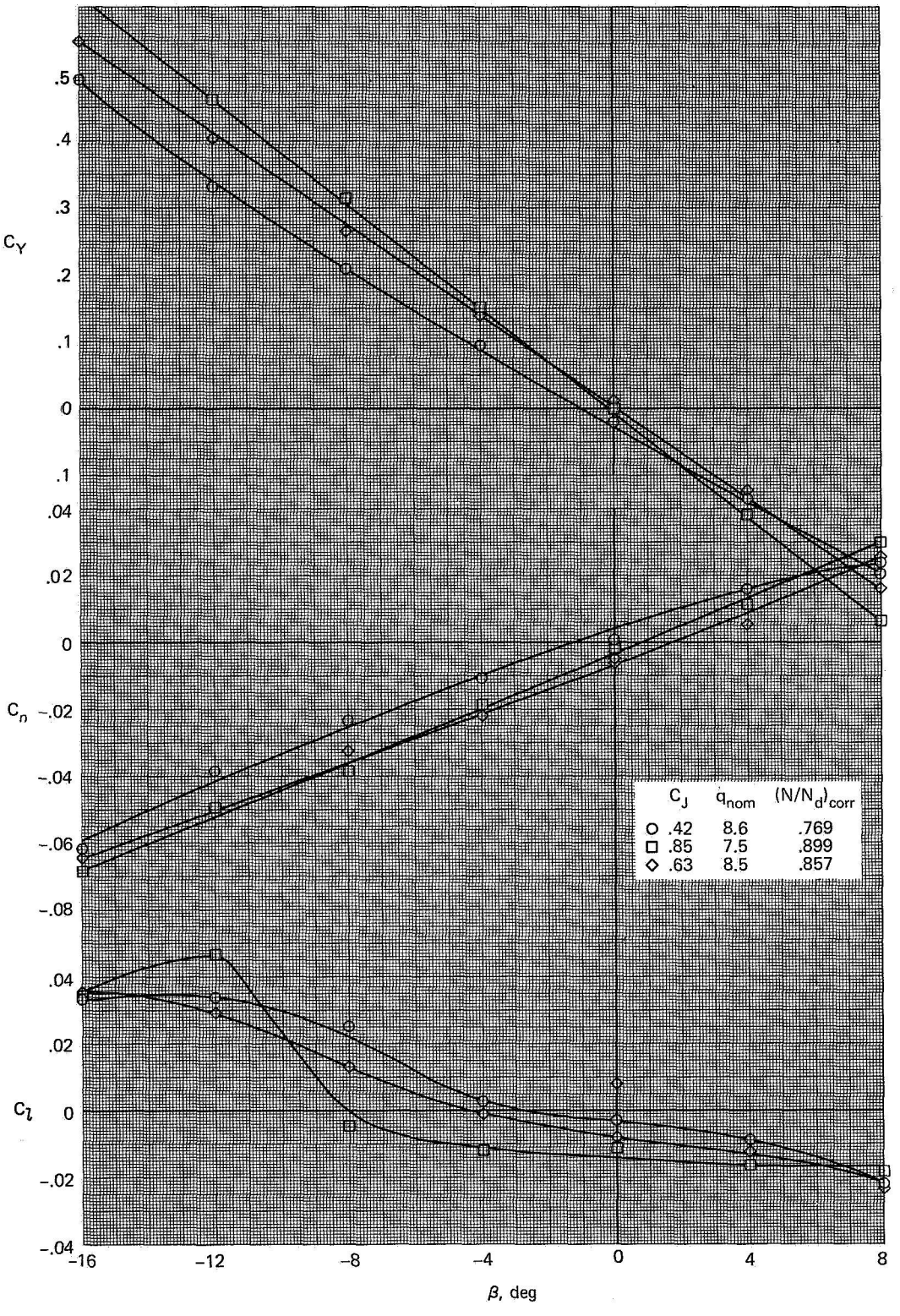

(c) $\delta_f = 30$, $\delta_a = 30/30$, $\alpha = 0$

Figure 15.– Continued.

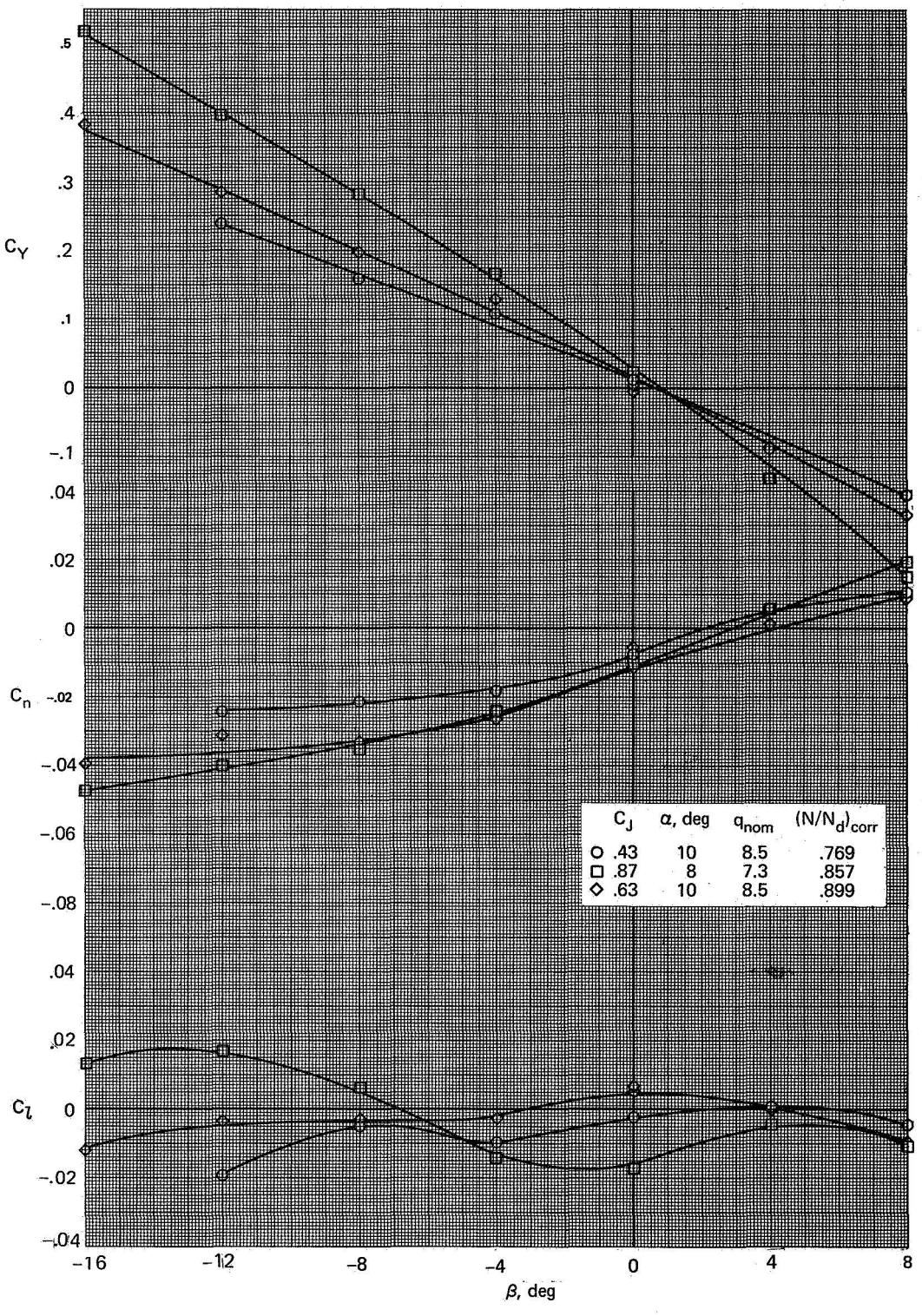

(d) $\delta_f = 30$, $\delta_a = 30/30$

Figure 15.– Concluded.

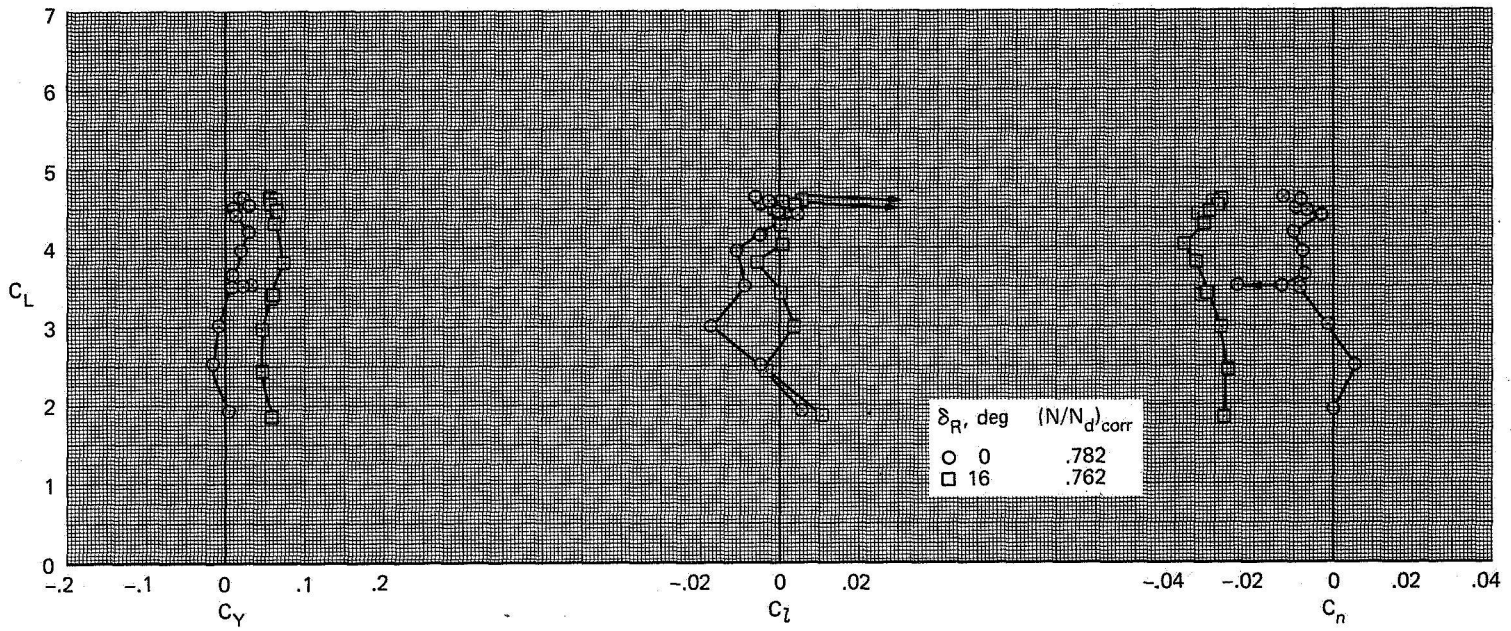

(a) $C_J = 0.43$, $q_{nom} = 8.5$

Figure 16.– The effect of rudder deflection on the lateral-directional characteristics of the aircraft; $\delta_f = 40$, $\delta_a = 40/40$, $i_t = 4$.

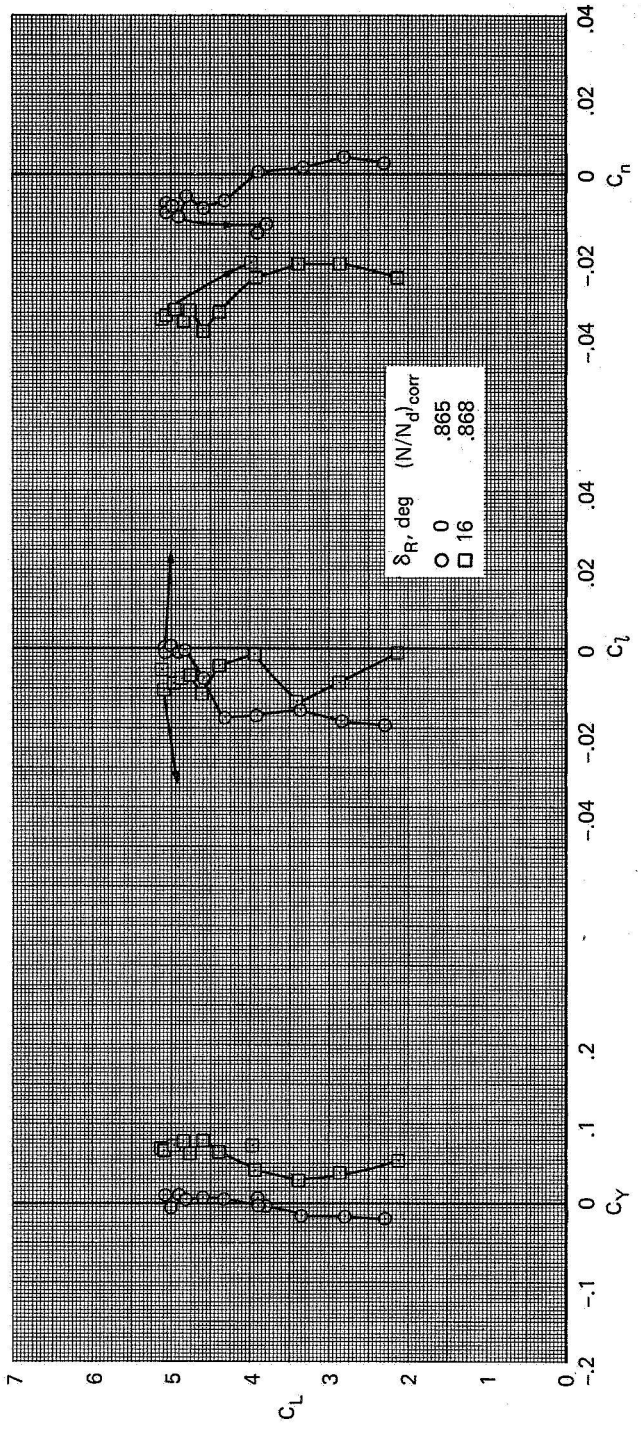

(b) $C_J = 0.63, q_{nom} = 8.5$

Figure 16.– Continued.

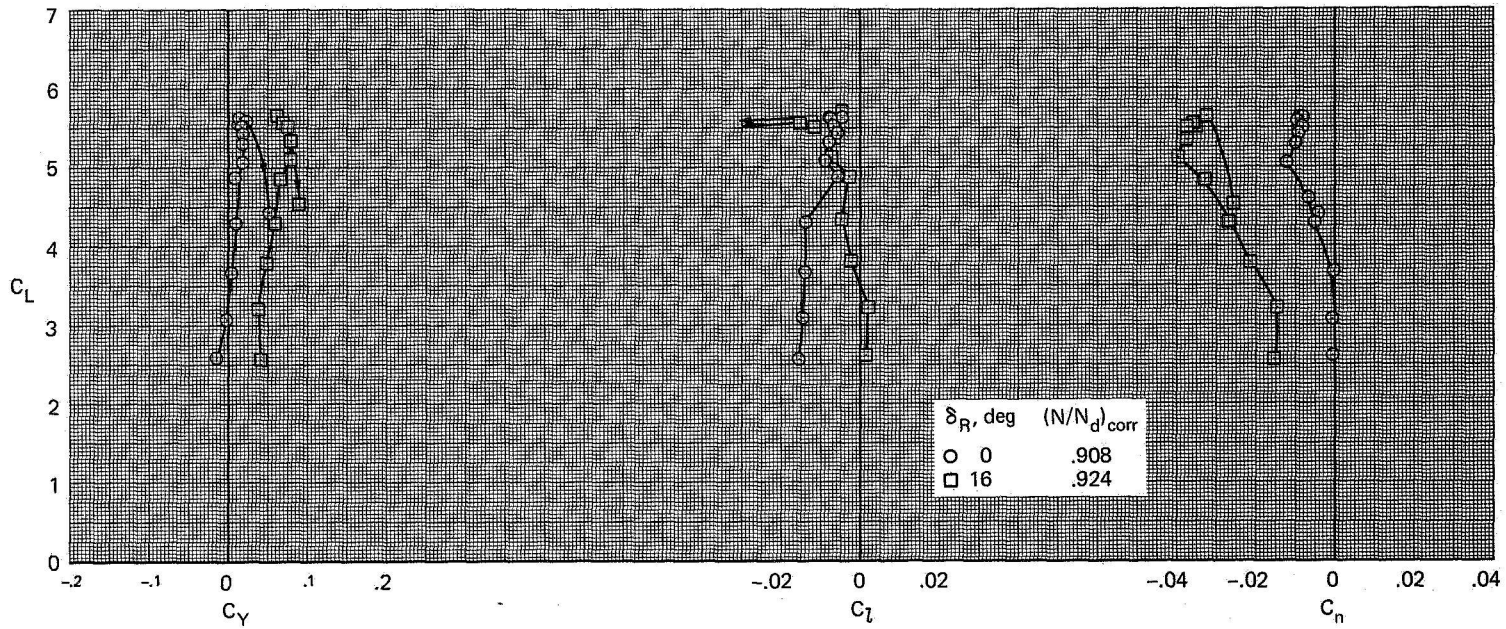

(c) $C_J = 0.87, q_{nom} = 7.3$

Figure 16.– Concluded.

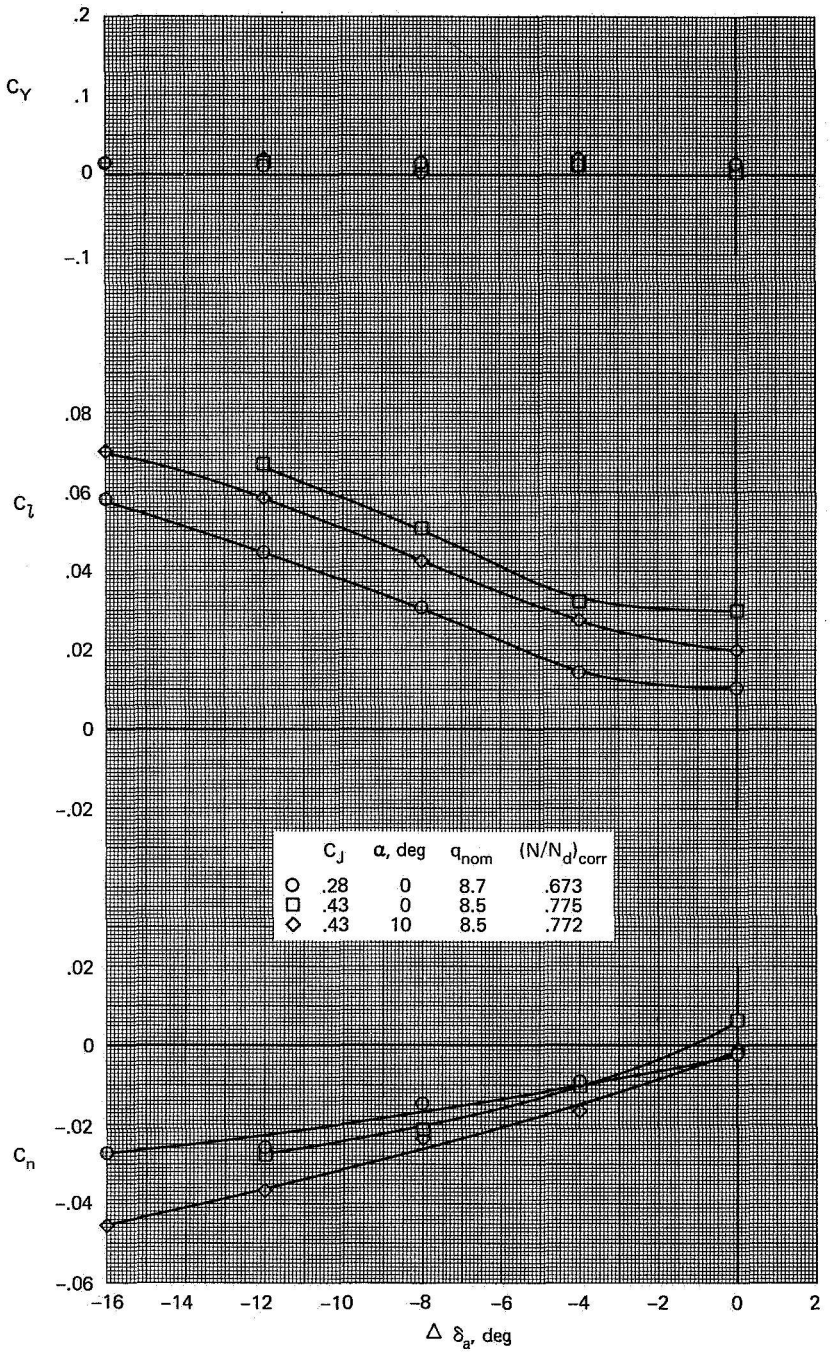

Figure 17.– The effects of C_J and angle of attack on the lateral-directional characteristics with varying asymmetric aileron deflection and roll jets on full right roll; $\delta_f = 40$, $\delta_{a_{nom}} = 40/40$, $i_t = -2$.

NASA-Langley, 1973 — 1 A–3611

NATIONAL AERONAUTICS AND SPACE ADMINISTRATION
WASHINGTON, D.C. 20546

OFFICIAL BUSINESS
PENALTY FOR PRIVATE USE $300

SPECIAL FOURTH-CLASS RATE BOOK

POSTAGE AND FEES PAID
NATIONAL AERONAUTICS AND SPACE ADMINISTRATION
451

U.S.MAIL

POSTMASTER: If Undeliverable (Section 158 Postal Manual) Do Not Return

"The aeronautical and space activities of the United States shall be conducted so as to contribute . . . to the expansion of human knowledge of phenomena in the atmosphere and space. The Administration shall provide for the widest practicable and appropriate dissemination of information concerning its activities and the results thereof."

—NATIONAL AERONAUTICS AND SPACE ACT OF 1958

NASA SCIENTIFIC AND TECHNICAL PUBLICATIONS

TECHNICAL REPORTS: Scientific and technical information considered important, complete, and a lasting contribution to existing knowledge.

TECHNICAL NOTES: Information less broad in scope but nevertheless of importance as a contribution to existing knowledge.

TECHNICAL MEMORANDUMS: Information receiving limited distribution because of preliminary data, security classification, or other reasons. Also includes conference proceedings with either limited or unlimited distribution.

CONTRACTOR REPORTS: Scientific and technical information generated under a NASA contract or grant and considered an important contribution to existing knowledge.

TECHNICAL TRANSLATIONS: Information published in a foreign language considered to merit NASA distribution in English.

SPECIAL PUBLICATIONS: Information derived from or of value to NASA activities. Publications include final reports of major projects, monographs, data compilations, handbooks, sourcebooks, and special bibliographies.

TECHNOLOGY UTILIZATION PUBLICATIONS: Information on technology used by NASA that may be of particular interest in commercial and other non-aerospace applications. Publications include Tech Briefs, Technology Utilization Reports and Technology Surveys.

Details on the availability of these publications may be obtained from:

SCIENTIFIC AND TECHNICAL INFORMATION OFFICE

NATIONAL AERONAUTICS AND SPACE ADMINISTRATION

Washington, D.C. 20546